

# On the association between core-collapse supernovae and H II regions

Paul A. Crowther<sup>★</sup>

*Department of Physics & Astronomy, University of Sheffield, Hicks Building, Hounsfield Road, Sheffield S3 7RH*

Accepted 2012 October 3. Received 2012 October 3; in original form 2012 August 7

## ABSTRACT

Previous studies of the location of core-collapse supernovae (ccSNe) in their host galaxies have variously claimed an association with H II regions; no association or an association only with hydrogen-deficient ccSNe. Here, we examine the immediate environments of 39 ccSNe whose positions are well known in nearby ( $\leq 15$  Mpc), low-inclination ( $\leq 65^\circ$ ) hosts using mostly archival, continuum-subtracted H $\alpha$  ground-based imaging. We find that 11 out of 29 hydrogen-rich ccSNe are spatially associated with H II regions ( $38 \pm 11$  per cent), versus 7 out of 10 hydrogen-poor ccSNe ( $70 \pm 26$  per cent). Similar results from Anderson et al. led to an interpretation that the progenitors of Type Ib/c ccSNe are more massive than those of Type II ccSNe. Here, we quantify the luminosities of H II region either coincident with or nearby to the ccSNe. Characteristic nebulae are long-lived ( $\sim 20$  Myr) giant H II regions rather than short-lived ( $\sim 4$  Myr) isolated, compact H II regions. Therefore, the absence of an H II region from most Type II ccSNe merely reflects the longer lifetime of stars with  $\lesssim 12 M_\odot$  than giant H II regions. Conversely, the association of an H II region with most Type Ib/c ccSNe is due to the shorter lifetime of stars with  $> 12 M_\odot$  stars than the duty cycle of giant H II regions. Therefore, we conclude that the observed association between certain ccSNe and H II provides only weak constraints upon their progenitor masses. Nevertheless, we do favour lower mass progenitors for two Type Ib/c ccSNe that lack associated nebular emission, a host cluster or a nearby giant H II region. Finally, we also reconsider the association between long gamma-ray bursts and the peak continuum light from their (mostly) dwarf hosts, and conclude that this is suggestive of very high mass progenitors, in common with previous studies.

**Key words:** stars: massive – supernovae: general – H II regions – galaxies: ISM.

## 1 INTRODUCTION

The past decade has seen major advances in establishing the progenitors of core-collapse supernovae (ccSNe; Smartt 2009). Three discrete subpopulations of hydrogen-rich ccSNe are known exhibiting plateau's (II-P), slow declines (II-L) and rapid declines (IIb) in their light curves (Arcavi et al. 2012), representing progressively lower hydrogen envelope masses. It has been empirically established that the most common of these (II-P) are the direct progeny of red supergiants (Smartt et al. 2009). Some of the rarer subtypes (II-L and IIb) have been proposed to originate from yellow supergiants, hydrogen-rich Wolf–Rayet stars or interacting binaries, while hydrogen-rich ccSNe with narrow components in their spectra (IIc) seem to involve interactions with dense circumstellar material (Kiewe et al. 2012).

No progenitors of hydrogen-deficient (Ib/c) ccSNe have yet been detected (Crockett et al. 2007; Yoon et al. 2012) which are believed to either arise from massive Wolf–Rayet stars that have stripped their

hydrogen from powerful stellar winds (e.g. Conti 1976; Crowther 2007), lower mass stars in close binary systems (Podsiadlowski, Joss & Hsu 1992; Nomoto, Iwamoto & Suzuki 1995; Fryer et al. 2007) or some combination thereof (Smith et al. 2011; Langer 2012). It is likely that helium-strong IIb and Ib ccSNe possess similar progenitor channels (Arcavi et al. 2012), while helium-weak Ic ccSNe may arise from disparate progenitors (e.g. Dessart et al. 2012). In particular, broad-lined Type Ic ccSNe are notable in several ways; they represent the majority of hydrogen-deficient ccSNe in dwarf hosts (Arcavi et al. 2010), there is a broad-lined Ic-gamma-ray burst (GRB) connection (Woolley & Bloom 2006), while long GRBs prefer metal-poor hosts (Levesque et al. 2010).

In view of the scarcity of nearby ccSNe amenable to the direct detection of the progenitor star, studies have turned to the host environment. For example, the population of hydrogen-deficient ccSNe are dominated by Ic ccSNe in large galaxies, versus Ib and broad-lined Ic ccSNe in dwarf galaxies (Arcavi et al. 2010), although the overall statistics of Ib/c versus II ccSNe are relatively insensitive to host galaxy.

In addition, the immediate environment from which the ccSNe originated has also been examined. The first serious attempt to

<sup>★</sup>E-mail: Paul.crowther@sheffield.ac.uk

assess their association with H II regions was by van Dyk (1992). From a sample of 38 ccSNe of all subtypes, he concluded that approximately 50 per cent were associated with an H II region, with no statistically significant difference between Type II and Ib/c SNe, albeit hampered by poor positional accuracy (up to  $\pm 10$  arcsec). Bartunov, Tsvetkov & Filimonova (1994) also concluded that both H-rich and H-deficient ccSNe were concentrated towards H II regions, implying similar ages/masses. Improved statistics (49 ccSNe) enabled van Dyk, Hamuy & Filippenko (1996) to confirm earlier results, concluding that the (massive) Wolf–Rayet scenario could be excluded for most Type Ib/c ccSNe, albeit once again subject to poor positional accuracy for many targets.

More recently, James & Anderson (2006), Anderson & James (2008) and Anderson et al. (2012) have taken a statistical approach to the environment of ccSNe, involving its position with respect to the cumulative distribution of H $\alpha$  emission in the host galaxy, whose recession velocities extended up to  $cz = 10\,000$  km s $^{-1}$ . Anderson & James (2008) found a low fraction of Type II SNe to be associated with H II regions, concluding that the ‘Type II progenitor population does not trace the underlying star formation’. In contrast, they noted that Type Ib, and especially Ic ccSNe are spatially coincident with H II regions, suggesting a progenitor mass sequence from II  $\rightarrow$  Ib  $\rightarrow$  Ic. Anderson et al. (2012) include additional statistics for hydrogen-rich ccSNe from which they claim a mass sequence II $\alpha$   $\rightarrow$  II-P  $\rightarrow$  II-L  $\rightarrow$  IIb. The latter naturally connects IIb and Ib ccSNe, but the low progenitor masses inferred for II $\alpha$  ccSNe does not readily match expectations that these arise from massive Luminous Blue Variables (LBV, Smith 2008).

To add to the puzzle, Smartt (2009) argued against a monotonic mass sequence for progenitors of II  $\rightarrow$  Ib  $\rightarrow$  Ic on the basis of the rate of Ib/c ccSNe, the lack of direct detections of Ib/c progenitors (e.g. Crockett 2009) and inferred low Ib/c ccSNe ejecta masses. From a qualitative study of the environment of the volume- and epoch-limited sample of ccSNe of Smartt et al. (2009), 0 from 17 Type II SN observed at high spatial resolution are located in bright H II regions (Smartt, private communication). Meanwhile, only 1 case from 9 Ib/c ccSNe from Crockett (2009) for which high spatial resolution imaging was available is located in a large star-forming region, albeit spatially offset from H II emission (Smartt, private communication). Therefore, high-resolution imaging does not appear to support any significant association between ccSNe and H II regions.

In addition to the association of ccSNe with H II regions, or lack thereof, studies of the location of ccSNe with respect to the host galaxy light have also been performed. Kelly, Kirschner & Pahre (2008) found that Type Ic ccSNe are located in the brightest regions of their host galaxies; Type II ccSNe are randomly distributed, with intermediate properties for Type Ib ccSNe. Long duration GRBs, in common with Type Ic ccSNe, are also strongly biased towards the brightest regions of their hosts (Fruchter et al. 2006), adding to the GRB-Ic SN link.

In this study, we re-assess the degree of association of nearby ccSNe with H II regions in their hosts, in an attempt to reconcile the recent Smartt (2009) and Anderson et al. (2012) studies. Section 2 provides a background to H II regions, star clusters and massive stars. Section 3 assesses the association of nearby ccSN with H $\alpha$  emission, while Section 4 looks into how/whether these results contribute to the question of progenitor masses for different flavours of ccSNe. In Section 5, we briefly re-assess the significance that certain ccSNe and long-duration GRBs are located in the brightest regions of their host galaxies, while brief conclusions are drawn in Section 6.

## 2 H II REGIONS AND MASSIVE STARS

In this section, we provide a brief background to the expected connections between massive stars and H II regions, of relevance to our empirical study set out in Section 3.

### 2.1 Clusters and massive stars

It is widely accepted that the majority of stars form within star clusters (Lada & Lada 2003), although recent evidence suggests that star formation occurs across a broad continuum of stellar densities (e.g. Evans et al. 2009) from dense star clusters to diffuse OB associations (Gieles & Portegies Zwart 2011). Nevertheless, given their short lifetimes (2.5–50 Myr) only a few per cent of massive stars ( $\geq 8 M_{\odot}$ ) appear genuinely ‘isolated’ (de Wit et al. 2005) such that they either tend to be associated with their natal cluster or are potential runaways from it.<sup>1</sup>

According to Weidner & Kroupa (2006), there is a tight relation between cluster mass, and the most massive star formed within the cluster, although this remains controversial (Calzetti et al. 2010; Eldridge 2012). If this is so, the galaxy-wide stellar initial mass function (IMF) will also depend upon the cluster mass function and the mass range spanned by star clusters (Pflamm-Altenburg, Weidner & Kroupa 2007). By way of example, a cluster with a mass of  $\sim 10^2 M_{\odot}$ , similar to the  $\rho$  Oph star-forming region (Wilking, Lada & Young 1989), will barely produce any massive stars. In contrast, a cluster with a stellar mass of  $10^4 M_{\odot}$ , such as NGC 3603 (Harayama, Eisenhauer & Martins 2008), would be expected to form  $\sim 100$  massive stars, with the most massive examples exceeding  $100 M_{\odot}$  (Schnurr et al. 2008; Crowther et al. 2010). Massive stars, therefore, tend to be intimately connected with the youngest, brightest star clusters.

### 2.2 H II regions: from classical to supergiant

In view of the Salpeter IMF slope for high-mass stars (Bastian, Covey & Meyer 2010), 8–20  $M_{\odot}$  early B-type stars form  $\sim 75$  per cent of their overall statistics. However, the most frequently used indicator of active star formation is nebular hydrogen emission (e.g. H $\alpha$ ) from gas ionized by young, massive stars. The Lyman continuum ionizing output from such stars is a very sensitive function of temperature (stellar mass), such that one O3 dwarf ( $\sim 75 M_{\odot}$ ) will emit more ionizing photons than 25 000 B2 dwarfs ( $\sim 9 M_{\odot}$ ; Conti, Crowther & Leitherer 2008). Therefore, H II regions are biased towards the  $\sim 25$  per cent of high-mass stars exceeding  $20 M_{\odot}$ , namely O-type stars (B stars will produce extremely faint H II regions).

Beyond several Mpc, current sensitivities limit the detection of H II regions to relatively bright examples, involving several ionizing early O-type stars (Pflamm-Altenburg et al. 2007). Still, the H $\alpha$  luminosity of bright H II regions can be converted into the corresponding number of Lyman continuum ionizing photons, for which the number of equivalent O7 dwarf stars,  $N(O7V)$ , serves as a useful reference (Vacca & Conti 1992). Table 1 lists examples of nearby H II regions (adapted from Kennicutt 1984, 1998) which range from classical H II regions powered typically by one or a few stars (e.g. M42), through giant, extended H II regions powered by tens of O stars (Carina Nebula) to exceptionally bright ‘supergiant’ regions

<sup>1</sup> Runaways may be ejected from their cluster either dynamically during the formation process or at a later stage after receiving a kick following a supernova explosion in a close binary system.

**Table 1.** Examples of nearby H II regions, spanning a range of luminosities, for an assumed O7V Lyman continuum ionizing flux of  $10^{49}$  (ph s $^{-1}$ ), adapted from Kennicutt (1984, 1998).

Region	Type	Galaxy	Distance (kpc)	Diameter (pc)	$L(\text{H}\alpha)$ (erg s $^{-1}$ )	$N(\text{O7V})$
Orion (M42)	Classical	Milky Way	0.5	5	$1 \times 10^{37}$	<1
Rosette (NGC 2244)	Classical	Milky Way	1.5	50	$9 \times 10^{37}$	7
N66	Giant	SMC	60	220:	$6 \times 10^{38}$	50
Carina (NGC 3372)	Giant	Milky Way	2.3	300:	$1.5 \times 10^{39}$	120
NGC 604	Giant	M33	800	400	$4.5 \times 10^{39}$	320
30 Doradus	Supergiant	LMC	50	370	$1.5 \times 10^{40}$	1100
NGC 5461	Supergiant	M101	6400	1000:	$7 \times 10^{40}$	5000

powered by hundreds of O stars (30 Doradus). We will follow these template H II regions when we investigate the nebular environment of ccSNe in Section 3. Although there is a spread in H II region size at a particular H $\alpha$  luminosity (e.g. Lopez et al. 2011, their fig. 1), faint regions are typically small ( $\leq 10$  pc), giant regions are extended ( $\sim 100$  pc) and supergiant regions tend to be very extended (several hundred pc).

Kennicutt, Edgar & Hodge (1989) have studied the behaviour of the H II region luminosity function in nearby spirals and irregular galaxies. Early-type (Sa-Sb) spirals possess a steep luminosity function, with the bulk of massive star formation occurring in small regions ionized by one of a few O stars (M42-like), plus a low cut-off to the luminosity function. Late-type spirals and irregulars possess a shallower luminosity function, in which most of the massive stars form within (30 Dor-like) large H II regions/OB complexes. For example, although the Large Magellanic Cloud (LMC) contains considerably fewer H II regions than M31 (SA[s]b), it contains 10 H II regions more luminous than any counterpart in M31 (Kennicutt et al. 1989).

### 2.3 Lifetime of H II regions

Before turning to our survey of nearby ccSNe, let us first assess the empirically determined duration of the H II region phase, for which both a plentiful supply of ionizing photons (from O stars) and neutral gas (left over from the star formation process) are required. The former is limited to  $\sim 10$  Myr according to the latest evolutionary model predictions for  $20 M_{\odot}$  stars (Ekström et al. 2012), and is often merely adopted as the H II lifetime, while the latter depends sensitively upon its environment. Walborn (2010) studied the properties of young, intermediate-mass star clusters within the Local Group which indicate that the H II region phase is present for only the first  $\sim 3$ – $4$  Myr. The gas is swept up and expelled via radiative and mechanical feedback from stars, and subsequently supernovae (e.g. Dale, Ercolano & Bonnell 2012).

Gas has already been removed from relatively high-mass, isolated clusters such as Westerlund 1 after 5 Myr ( $\sim 10^5 M_{\odot}$ ; Clark et al. 2005). Therefore, one would *not* expect ccSNe to be spatially coincident with *isolated* H II regions unless the mass of the progenitor was sufficiently high ( $> 75 M_{\odot}$ ) for its lifetime to be comparable to the gas dispersion time-scale.

This is illustrated in Fig. 1(a) where we compare the lifetime of the most massive stars in clusters<sup>2</sup> (according to equation 10 from Pflamm-Altenburg et al. 2007), with an estimate of the duration of isolated H II regions (adapted from Walborn 2010). Solely very

massive ( $> 75 M_{\odot}$ ) stars would end their life before the gas in the associated H II region had dispersed.

Of course, not all massive star formation occurs within isolated, compact star clusters. Giant and supergiant H II regions extending to several hundred parsec in size (Table 1) are ionized by successive generations of star clusters, with a total duty cycle of  $\sim 20$  Myr. Therefore, older (lower mass) populations will appear co-located with younger (higher mass) stars in external (super)giant H II regions. Indeed, 30 Doradus would only subtend  $\sim 1$  arcsec at a distance of 50 Mpc.

For giant H II regions, such as the Carina Nebula, several clusters exist with distinct ages, ranging from 1–2 Myr (Trumpler 14; e.g. Vazquez et al. 1996) to 5–10 Myr (Trumpler 15; e.g. Wang et al. 2011). Indeed, the proximity of the supergiant H II region 30 Doradus enables individual stars to be studied in detail (e.g. Evans et al. 2011). Walborn & Blades (1997) identified five distinct spatial structures within 30 Dor: (i) the central 1–2 Myr cluster R136; (ii) a surrounding triggered generation embedded in dense knots ( $< 1$  Myr); (iii) an OB supergiants spread throughout the region (4–6 Myr); (iv) an OB association with the southeast surrounding R143 ( $\sim 5$  Myr); (v) an older (20–25 Myr) cluster to the northwest (Hodge 301; Grebel & Chu 2000).

Therefore, a massive star from the first stellar generation exploding within such an environment as an SN after 5–10+ Myr would still be associated with a bright H II region, even if its natal star cluster had cleared the gas from its immediate vicinity, as illustrated in Fig. 1(b). A total duty cycle of 20 Myr for giant H II regions sets a lower threshold of  $12 M_{\odot}$  to the progenitor mass (from the initial stellar generation) for possible association with the giant H II region. Progressively higher mass progenitors from subsequent generations (for illustration, four generations separated by 5 Myr are shown in Fig. 1b) would be required. For example, a star formed 10 Myr after the initial burst would only be associated with the giant H II region if its initial mass exceeded  $20 M_{\odot}$ .

Finally, (nuclear) starburst regions of galaxies, in which gas is continuously accreted, may have still longer duty cycles of  $\sim 100$  Myr, preventing any constraints upon progenitor masses.

In summary, we set out five scenarios, depending on whether or not the ccSNe are spatially coincident with H II regions, as follows.

(i) Class 1: the ccSNe progenitor is coincident with an isolated, young, bright star cluster from which the gas has been expelled, so an H II region is *absent*. At optical wavelengths, a star cluster rapidly fades (by 1 mag) at early times between 5 and 10 Myr, with a slower decline of 0.5 mag between 10 and 30 Myr (e.g. Bik et al. 2003), so that a high-mass progenitor ( $\geq 20 M_{\odot}$ ) might be anticipated.

(ii) Class 2: either the ccSNe progenitor is coincident with an isolated, faint star cluster or is not coincident with any detectable star cluster. In this case, the cluster may have already dissolved

<sup>2</sup> Stellar lifetimes are adopted from rotating, solar metallicity models of Ekström et al. (2012).

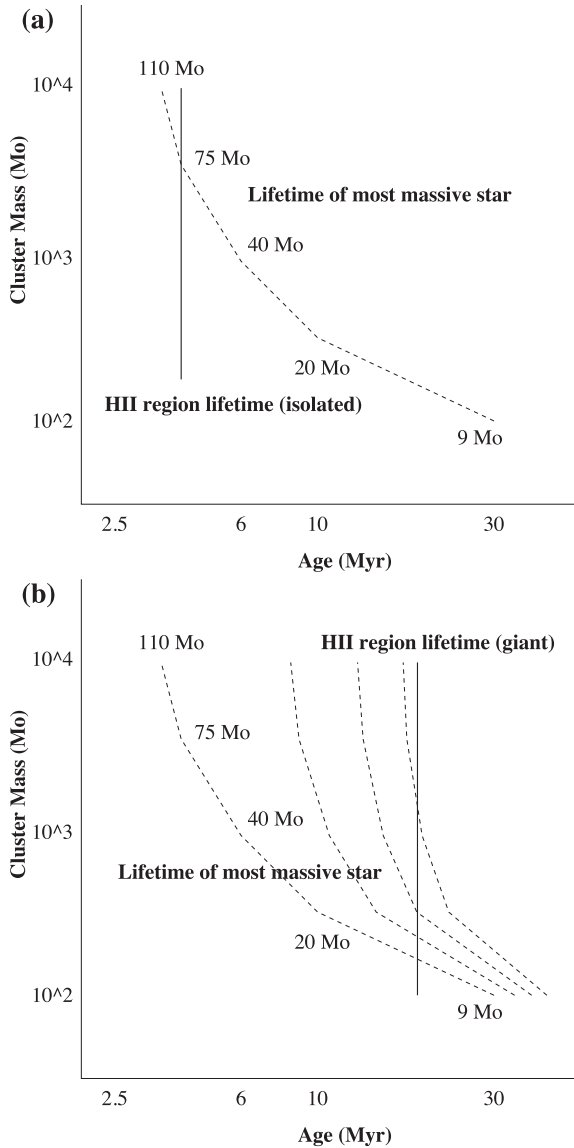


**Figure 1.** (a) Schematic comparing the lifetime of the most massive star in a cluster (dotted line, according to Pflamm-Altenburg et al. 2007) and isolated H II regions (vertical solid line, adapted from Walborn 2010). ccSNe should only be associated with isolated H II regions for very massive progenitors; (b) the same as (a) except for (super)giant H II regions, comprising four distinct star-forming episodes separated by 5 Myr, with the age referring to the first stellar generation. For a total duty cycle of 20 Myr, an association between ccSNe and giant H II regions would be expected except for progenitors with masses below  $\sim 12 M_{\odot}$  or more massive progenitors from subsequent stellar generations as indicated.

and an H II region again *absent*. This scenario would favour an older ( $\gg 10$  Myr) cluster, and correspondingly lower mass progenitor ( $< 20 M_{\odot}$ ).

(iii) Class 3: the ccSNe progenitor was formed in a star cluster, but was subsequently ejected via either dynamical interactions or after receiving a kick from the supernova of a close companion, so it is not directly associated with an H II region, although a bright H II region is *nearby*. For a dynamical interaction origin, if a massive star has a space velocity of  $50 \text{ km s}^{-1}$  with respect to its natal cluster, typical of a runaway, its projected distance would be up to 150 pc after 3 Myr or 1.5 kpc after 30 Myr. According to Fujii &

Portegies Zwart (2011) the fraction of dynamical runaways is low ( $< 0.1$  per cent) for high-mass ( $10^5 M_{\odot}$ ) star clusters, but increasing to 1–10 per cent for high-mass stars in less massive ( $10^4 M_{\odot}$ ) clusters. Therefore, one would anticipate a nearby (few hundred pc), high-mass, dense star cluster, given the short lifetime of high-mass ( $\geq 25 M_{\odot}$ ) stars, which would most likely lie within a giant H II region (e.g. Carina Nebula, 30 Doradus).

(iv) Class 4: an H II region is *present* at the ccSNe position, albeit with a low luminosity. This favours a very high mass progenitor ( $> 75 M_{\odot}$ ) if the star-forming region is compact/isolated, or a significantly lower mass ( $\leq 20 M_{\odot}$ ) if it is merely an older, extended star-forming region.

(v) Class 5: an H II region is again *present* at the ccSNe position, albeit spatially extended, with a high luminosity. The progenitor was formed in a cluster within a large star-forming complex in which ongoing star formation is maintaining the Lyman continuum radiation. The natal cluster may be detected, it could have already dissolved, or the star could be a runaway from a nearby high-mass cluster. For a giant H II region duty cycle of 20 Myr, a lower limit of  $12 M_{\odot}$  can be assigned for a progenitor formed in the first generation of stars, with an increasing mass limit for subsequent generations (recall Fig. 1b). If the ccSNe is associated with a very long lived starburst region, no robust limit to the progenitor mass can be assigned.

### 3 ARE CCSNE ASSOCIATED WITH H II REGIONS?

In this section, we discuss the supernova sample investigated, together with methods used and re-assess whether nearby ccSNe are associated with H II regions in their host galaxy.

#### 3.1 Supernova sample

Here, we examine the association of ccSNe with H II regions in their host galaxies. We follow an approach broadly similar to van Dyk (1992) and van Dyk et al. (1996). This technique is complementary to qualitative approaches (Crockett 2009; Smartt, private communication) and the cumulative distribution technique of James & Anderson (2006), Anderson & James (2008) and Anderson et al. (2012).

We limit our sample to local, historical, non-type Ia SNe from the Asiago Catalogue<sup>3</sup> with a cut-off date of 2012 March 31. Ground-based images used in this study have a spatial resolution of 0.6–4 arcsec, aside from the LMC, so we set an upper limit of 15 Mpc for ccSNe host galaxies, at which the typical image quality (FWHM  $\sim 1.5$  arcsec) corresponds to the radius of a giant H II region ( $\sim 100$  pc). Distances are uniformly obtained from the Extragalactic Distance Database (EDD; Tully et al. 2009). For reference, Tables B1–B2 (online-only; see Supporting Information) in Appendix B list ccSNe host galaxies for which EDD distances lie in the 15–20 Mpc range.

In total 88 ccSNe within 15 Mpc are listed in the Asiago Catalogue, from which 11 were removed on the basis that they are believed to be SN imposters or LBV eruptions.<sup>4</sup> We also omit 21 ccSNe for which merely offsets relative to the centre of host galaxy are known, although we retain historical SNe whose positions are known to a precision of  $\sim 1$  arcsec.

<sup>3</sup> <http://graspa.oapd.inaf.it>

<sup>4</sup> SN 1954J, 1961V, 1978K, 1997bs, 1999bw, 2000ch, 2002kg, 2002bu, 2008S, 2010da and 2010dn.

**Table 2.** Properties of Type Ib/c ccSNe used in this study, including deprojected spectral types (column 2), host galaxies (column 3), distance (column 4), positions (columns 5–6, from Asiago Catalogue except where noted), deprojected galactocentric distances (column 7,  $R_{\text{SN}}$ ), source of H $\alpha$  imaging (column 8, key in Table 5), whether the SN is associated with a cluster (column 9) or nebular emission (column 10), including results from *HST* imaging in parentheses. Column 11 provides information on the closest H II region, including its offset and deprojected distance from the SN and whether it is spatially extended (ext.) or compact (comp.). Columns 12–14 present, respectively, the flux ( $F$ ,  $\leq \pm 0.1$  dex), radius ( $r$ ,  $\pm 0.5$  arcsec) and H $\alpha$  luminosity ( $L$ , factor of 2) of the H II region, while column 15 shows the class of environment.

SN	SN type	Host	$d$ Mpc	SN (J2000) $\alpha, \delta$		$R_{\text{SN}}$ $R_{25}$	Tel ID	Cl? ( <i>HST</i> )	H $\alpha$ ? ( <i>HST</i> )	Comment	$F(\text{H}\alpha + [\text{N II}])$ erg s $^{-1}$ cm $^{-2}$	$r(\text{H II})$ arcsec	$L(\text{H}\alpha)$ 10 $^{37}$ erg s $^{-1}$	Class
1983N <sup>1</sup>	Ib	M83	4.92	13 36 51.28	−29 54 02.8	0.48	j1	✗	✓	Ext. H II reg. 1 arcsec/25 pc E	$6 \times 10^{-15}$	1.5	3	4
1985F	Ib/c	NGC 4618	9.2	12 41 33.01	+41 09 05.9	0.10	i	✓	✓	Twin GH II reg. 8 arcsec/180 pc SE Coincident w GH II reg.	$1.4 \times 10^{-13}$ $5 \times 10^{-14}$	5 2.5	80 46	5
1994I	Ic	M51a	8.39	13 29 54.07	+47 11 30.5	0.06	h	✗	✓	Ext. GH II reg. 2 arcsec/80 pc W	$1.0 \times 10^{-14}$	2	13	5
1997X	Ib	NGC 4691	12.0	12 48 14.28	−03 19 58.5	0.14	11	✗	✗	Ext. GH II reg. 9 arcsec/0.38 kpc SW H II reg. 1.5 arcsec/100 pc SW (Giant) H II reg. 6 arcsec/0.4 kpc SSW	$2 \times 10^{-14}$	2	30	– – –
2002ap	Ic	M74	9.0	01 36 23.85	+15 45 13.2	0.89	e1,n	✗	✗	Ext. H II 10 arcsec/400 pc SE	$2 \times 10^{-15}$	4	2	2
2003jg	Ib/c	NGC 2997	11.7	09 45 37.91	−31 11 21.0	0.07	f	✗	✗	Ext H II reg. 2 arcsec/140 pc E Nuclear starburst 12 arcsec/650 pc E	$1.2 \times 10^{-15}$ $7 \times 10^{-13}$	1.5 10	4 2200	2
2005at	Ic	NGC 6744	11.6	19 09 53.57	−63 49 22.8	0.30	j1	✓	✓	Coincident with ext. H II reg.	$2 \times 10^{-15}$	1.5	7	4
2005kl	Ic	NGC 4369	11.2	12 24 35.68	+39 23 03.5	0.17	m	✗	✓	(Giant?) H II reg. 1.5 arcsec/80 pc SE	–	2	–	5
2007gr	Ic	NGC 1058	9.86	02 43 27.98	+37 20 44.7	0.45	i	✓	✓	Ext. H II reg. 1.5 arcsec/75 pc NE	$1.1 \times 10^{-14}$	2	16	5
2008eh	Ib/c?	NGC 2997	11.3	09 45 48.16	−31 10 44.9	0.50	f	✗	✓	Ext. GH II reg. 2 arcsec/100 pc W Edge of GH II reg. Ext. GH II reg. 4.5 arcsec/250 pc S	$4 \times 10^{-14}$ $1.2 \times 10^{-14}$ $2 \times 10^{-14}$	2.5 2 2.5	60 40 70	– – –

1: SN 1983N coordinates from Sramek, Panagia & Weiler (1984).

Finally, we exclude 15 additional SNe whose host galaxies are observed at high inclination ( $\geq 65^\circ$ ) owing to the potential for confusion with unrelated line-of-sight H II regions. Inclinations were obtained from HyperLeda,<sup>5</sup> such that 41 ccSNe meet our criteria. Basic properties of these ccSNe are listed in Tables 2 and 3 for Type Ib/c and Type II ccSNe, respectively, with positions adopted from Asiago except where noted.

Uncalibrated H $\alpha$  images were available for NGC 4369 and NGC 4691, while no H $\alpha$  observations of either NGC 2082 or UGC 12160 were available. Therefore, the final sample comprises 39 SNe, subdivided into 29 Type II and 10 Type Ib/c ccSNe. Basic properties of the SN host galaxies are presented in Table 4, which include high-inclination galaxies (shown in bold) plus hosts lacking accurate ccSNe coordinates (shown in italics).

### 3.2 H $\alpha$ data sets of ccSNe host galaxies

We have examined the immediate environment of these 41 ccSNe in their 30 host galaxies using (primarily) archival, continuum-subtracted H $\alpha$  (+[N II]) imaging. Calibrated images are available for 37 ccSNe, uncalibrated images are available for SN 1997X (NGC 4691) and SN 2005kl (NGC 4369) from the 2.0 m Liverpool Telescope and 2.5 m Isaac Newton Telescope, respectively. We exclude SN 1992ba (NGC 2082) and SN 1995X (UGC 12160) from our global statistics since no H $\alpha$  images of their host galaxies are publically available, although we discuss literature descriptions for these cases. Therefore, in 39 cases we have examined the association between ccSNe with H II regions, and in 37 cases measured nebular fluxes and converted these into H $\alpha$  luminosities. In view of the possibility that the SN progenitor may have been ejected from its birth cluster, we examine the environment to typical projected distances of 0.5 kpc.

Table 5 indicates the source of the continuum-subtracted H $\alpha$  images used in our study. The majority of archival images were provided in flux-calibrated format, for which the 11 Mpc H $\alpha$  and UV Survey (11HUGS, Kennicutt et al. 2008) and Spitzer Infrared Nearby Galaxy Survey (SINGS, Kennicutt et al. 2009)<sup>6</sup> alone enabled the nebular environment of 40 per cent of the ccSNe to be assessed. The majority of the remaining host galaxies were included in other H $\alpha$  surveys of nearby galaxies, namely H $\alpha$  Galaxy Survey (H $\alpha$ GS) (James et al. 2004), Survey for Ionization in Neutral Gas Galaxies (SINGG, Meurer et al. 2006) and those by Hoopes et al. (2001) and Knapen et al. (2004). For M101, we used the low-resolution, flux-calibrated 0.6 m Kitt Peak National Observatory (KPNO) Schmidt imaging by Hoopes et al. (2001) together with higher spatial resolution, uncalibrated 2.5 m Isaac Newton Telescope (INT)/Wide Field Camera (WFC) imaging obtained from the ING archive,<sup>7</sup> which was also used in several other cases (e.g. NGC 7292). We have also inspected *Hubble Space Telescope* (*HST*) WFPC2, ACS and WFC3 imaging from the ESA Hubble Science Archive,<sup>8</sup> which is available for a subset of the ccSNe. The Hubble Heritage Team ACS/WFC mosaic of M51a was obtained from a dedicated website.<sup>9</sup> Narrow-band H $\alpha$  imaging is only available for eight ccSNe from our sample, while broad-band images have been obtained in 22 cases, the latter relevant for the potential association with compact star clusters.

NGC 2997, NGC 1559 and the LMC host the remaining four ccSNe omitted from these H $\alpha$  surveys. For the LMC, we employ continuum-subtracted H $\alpha$  imaging obtained with a Nikon survey

<sup>6</sup> Available from Local Volume Legacy Survey (LVLS) at <http://www.ast.cam.ac.uk/research/lvls>

<sup>7</sup> <http://casu.ast.cam.ac.uk/casuadc/archives/ingarch>

<sup>8</sup> <http://archives.esac.esa.int/hst/>

<sup>9</sup> <http://archive.stsci.edu/prepds/m51/>

<sup>5</sup> <http://leda.univ-lyon1.fr>

**Table 3.** Properties of Type II ccSNe used in this study. Column headings are as in Table 2.

SN	SN type	Host	$d$ (Mpc)	SN (J2000) $\alpha, \delta$	$R_{SN}$ $R_{25}$	Tel ID	CI? ( <i>HST</i> )	H $\alpha$ ? ( <i>HST</i> )	Comment	$F(\text{H}\alpha + [\text{N II}])$ $\text{erg s}^{-1} \text{cm}^{-2}$	$r(\text{H II})$ arcsec	$L(\text{H}\alpha)$ $10^{37} \text{erg s}^{-1}$	Class
1923A	II-P:	M83	4.92	13 37 09.2 −29 51 04	0.33	j1	X (X)	✓? (✓)	Ext. GH II reg. $\sim 4$ arcsec/100 pc N	$3 \times 10^{-14}$	4	78	5
1964H <sup>5</sup>	II	NGC 7292	12.9	22 28 24.06 +30 17 23.3	0.51	d2,i2	X (X)	X (X)	H II reg. 5 arcsec/0.35 kpc NW GH II reg. 7 arcsec/0.5 kpc W	$1.4 \times 10^{-15}$ $4 \times 10^{-15}$	2 2	4 13	2
1968D	II	NGC 6946	7.0	20 34 58.32 +60 09 34.5	0.14	k	X (X)	X (X)	H II reg. 4.3 arcsec/150 pc SSE Ext. H II reg. 12 arcsec/400 pc NNE	$5 \times 10^{-15}$ $1.1 \times 10^{-14}$	2 3	3 7	2
1968L	II-P	M83	4.92	13 37 00.51 −29 51 59.0	0.02	j1	X (X)	✓ (✓)	GH II reg. 1 arcsec/25 pc E Double GH II reg. 3 arcsec/75 pc N	$3 \times 10^{-13}$ $2 \times 10^{-12}$	1 2	150 1200	5
1970G <sup>5</sup>	II-L	M101	6.96	14 03 00.76 +54 14 33.2	0.46	b,i2	✓ (X)	✓ (X?)	Edge of GH II reg.	$2 \times 10^{-12}$	20	2070	5
1980K	II-L	NGC 6946	7.0	20 35 30.07 +60 06 23.7	0.99	h	X (X)	X (X?)	H II reg. 60 arcsec/2.1 kpc WNW	$6 \times 10^{-15}$	2	4	2
1986L <sup>5</sup>	II-L	NGC 1559	12.6	04 17 29.4 −62 47 01	0.55	j2	X (X)	X (X)	H II reg. 2 arcsec/150 pc N GH II reg. 3 arcsec/230 pc SW	$2 \times 10^{-15}$ $3 \times 10^{-14}$	1 2	8 95	3
1987A	Ipec	LMC	0.05	05 35 28.01 −69 16 11.6	–	a1,a2	X <sup>1</sup>	✓	H II complex 2.75 arcmin/40 pc NW GH II reg. 20.5 arcmin/300 pc NE	$1.3 \times 10^{-10}$ $1.4 \times 10^{-8}$	2 arcmin 10.5 arcmin	7 735	4
1992ba	II	NGC 2082	13.1	05 41 47.1 −64 18 00.9	0.55			2					
1993J	Iib	M81	3.6	09 55 24.95 +69 01 13.4	0.32	h	X (X)	SNR? (SNR)	Coincident with faint emission Ext. H II reg. 21 arcsec/580 pc NE	$1.1 \times 10^{-15}$ $1.1 \times 10^{-14}$	2 3	0.1 1.3	2
1995V	II-P	NGC 1087	14.4	02 46 26.77 −00 29 55.6	0.36	d2	X?	X?	GH II reg. 5 arcsec/0.6 kpc SW	$5 \times 10^{-15}$	3.5	18	2
1995X	II	UGC 12160	14.4	22 40 51.30 +75 10 11.5	0.42			3					
1996cr	IIn:	Circinus	4.21	14 13 10.01 −65 20 44.4	0.18	c	X (X)	✓ (✓)	GH II reg. 3 arcsec/100 pc SE Ext. GH II reg. 15 arcsec/0.5 kpc NNW	$3 \times 10^{-14}$ $7 \times 10^{-14}$	4 5	31 67	5
1998dn	II	NGC 337A	11.4	01 01 27.08 −07 36 36.7	1.21	d1	X (X)	X (X)	Bright H II reg. 5.5 arcsec/500 pc NW H II reg. 6 arcsec/300 pc SE	$5 \times 10^{-14}$ $7 \times 10^{-16}$	2.5 2	14 1.6	3 2
1999em <sup>5</sup>	II-P	NGC 1637	9.77	04 41 27.05 −02 51 45.8	0.22	e1	X (X)	X (X)	H II reg. 9.5 arcsec/0.5 kpc SE	$7 \times 10^{-15}$	3	15	
1999eu	II-P	NGC 1097	14.2	02 46 20.79 −30 19 06.1	0.83	e2	X (X)	X (X)	H II reg. 3.75 arcsec/375 pc W	$8 \times 10^{-16}$	2	8	2
1999gi	II-P	NGC 3184	13.0	10 18 16.66 +41 26 28.2	0.28	h	X? (X)	✓ (X?)	Ext. H II reg. 2 arcsec/125 pc SW Ext. H II reg. 2 arcsec/125 pc NE	$3 \times 10^{-15}$ $9 \times 10^{-15}$	2 3	8 22	5
2001X <sup>5</sup>	II-P	NGC 5921	14.0	15 21 55.46 +05 03 43.1	0.34	d2	X (X)	X (X)	Diffuse H II reg. 3 arcsec/0.3 kpc SE Ext. H II reg. 4 arcsec/0.4 kpc N	$3 \times 10^{-15}$ $9 \times 10^{-15}$	2 2	12 36	3
2001ig	Iib	NGC 7424	7.94	22 57 30.69 −41 02 25.9	1.02	e1	X (X)	✓ (X)	Edge of ext. H II reg.	$1.5 \times 10^{-15}$	2.5	2	4
2002hh <sup>5</sup>	II-P	NGC 6946	7.0	20 34 44.25 +60 07 19.4	0.38	k	X (X)	✓ (SNR)	Ext. GH II reg. 2.5 arcsec/85 pc NW	$4 \times 10^{-14}$	4	26	5
2003B	II-P	NGC 1097	14.2	02 46 13.78 −30 13 45.1	1.04	e2	X (X)	✓ (X)	Edge of ext. GH II reg. H II reg. 7 arcsec/300 pc SW	$6 \times 10^{-15}$ $2 \times 10^{-15}$	3 1.5	58 2	5 2
2003gd	II-P	M74	9.0	01 36 42.65 +15 44 19.9	0.51	j1	X (X)	X (X?)	Ext. GH II reg. 12 arcsec/500 pc SW	$2 \times 10^{-14}$	5	20	
2004dj	II-P	NGC 2403	3.16	07 37 17.02 +65 35 57.8	0.34	h <sup>4</sup>	✓ (X)	X (X)	Ext. H II reg. 21 arcsec/450 pc NW Ext. GH II reg. 21 arcsec/450 pc SE	$4 \times 10^{-14}$ $5 \times 10^{-13}$	2.5 7.5	6 73	1
2004et	II-P	NGC 6946	7.0	20 35 25.33 +60 07 17.7	0.82	h	X (X)	X (X?)	Ext. H II reg. 9 arcsec/300 pc N	$3 \times 10^{-15}$	2	2	2
2005cs	II-P	M51a	8.39	13 29 52.85 +47 10 36.3	0.30	h	✓? (X)	✓ (X)	Ext. H II reg. 1 arcsec/40 pc E Ext. GH II reg. 13 arcsec/0.55 kpc E	$1.4 \times 10^{-15}$ $1.0 \times 10^{-14}$	1.5 2	2 13	4
2008bk	II-P	NGC 7793	3.61	23 57 50.42 −32 33 21.5	0.75	e2	X (X)	X (X)	H II reg. 7 arcsec/200 pc SW	$1.8 \times 10^{-14}$	3	5	2
2009N	II-P	NGC 4487	11.0	12 31 09.46 −08 02 56.3	0.77	d1	X (X)	X (X)	Comp. H II reg. 3 arcsec/200 pc NW Ext. H II reg. 3 arcsec/200 pc NE	$8 \times 10^{-16}$ $3 \times 10^{-15}$	1.5 2.5	2 6	2
2009ib	II-P	NGC 1559	12.6	04 17 39.92 −62 46 38.7	0.67	j2	X (✓)	X (X?)	Ext. H II reg. 1.5 arcsec/170 kpc SE Ext. GH II reg. 6 arcsec/0.7 kpc SW	$3 \times 10^{-15}$ $1.3 \times 10^{-14}$	1 1.5	9 40	2
2011dh	Iib	M51a	8.39	13 30 05.12 +47 10 11.3	0.50	h	X (X)	✓ (X)	Bright H II reg. 8 arcsec/0.35 kpc SE Ext. GH II reg. 11 arcsec/0.5 kpc NE	$5 \times 10^{-15}$ $1.0 \times 10^{-14}$	2 3	7 14	2
2012A	II-P	NGC 3239	10.0	10 25 07.39 +17 09 14.6	0.42	g	X (X)	✓ (X)	Edge of H II reg. Ext. GH II reg. 10 arcsec/0.6 kpc NE	$6 \times 10^{-15}$ $4 \times 10^{-13}$	2 4	9 525	4
2012aw	II-P	M95	10.0	10 43 53.76 +11 40 17.9	0.62	h	X (X)	X (X)	H II reg. 5 arcsec/260 pc NNE H II reg. 10 arcsec/525 pc SW	$4 \times 10^{-16}$ $1.2 \times 10^{-15}$	2 2	0.6 2	2

1: SN 1987A is associated with a faint cluster (Panagia et al. 2000) that would be not detected at the typical distance of the other ccSNe.

2: SN 1992ba is located within or close to a bright H II region according to Schmidt et al. (1994).

3: SN 1995X is located close to the maximum H $\alpha$  brightness of UGC 12160 according to Anderson et al. (2012).

4: KPNO 2.1 m H $\alpha$  imaging of Kennicutt et al. (2003) is supplemented by continuum-subtracted NOT/ALFOSC H $\alpha$  imaging from Larsen & Richtler (1999).

5: Coordinates: SN 1964H (Porter 1993); SN 1970G (Allen et al. 1976); SN 1986L (McNaught & Waldron 1986); SN 1999em (Jha et al. 1999); SN 2001X (Li et al. 2001); SN 2002hh (Stockdale et al. 2002).

camera plus 2K CCD (Bessell, private communication), lower resolution Parking Lot Camera (PLC) H $\alpha$  and  $R$ -band images from Bothun & Thompson (1988) and Kennicutt et al. (1995), plus higher resolution Magellanic Cloud Emission Line Survey (MCELS) imaging of 30 Doradus obtained using the Cerro Tololo Inter-

American Observatory (CTIO) Curtis Schmidt telescope (Smith, Leiton & Pizarro 2000). For NGC 2997, we have resorted to the Danish 1.5 m observations of Larsen & Richtler (1999). For NGC 1559, we have used high spatial resolution archival Very Large Telescope (VLT)/FORIS1 imaging [from 075.D-0213(A), PI D. Baade].

**Table 4.** Basic properties of host galaxies of ccSNe used in this study (within 15 Mpc), drawn from RC3 or HyperLeda. Hosts viewed at unfavourable high inclinations ( $\geq 65^\circ$ ) were excluded from the study, but are listed (in bold) separately, as are hosts of ccSNe excluded owing to imprecise SN positions (in italics).

PGC	M	NGC	UGC	Type	$cz$ (km s $^{-1}$ )	$i$	PA	$d$ (Mpc)	Ref mag	$m_{B_T}$ (mag)	$A_B$ (mag)	$M_{B_T}$	ccSNe	
03671		337A		SAB(s)dm	1074	56.1	8	11.4	± 2.1	1	12.70	0.35	-17.94	1998dn
05974	74	628	01149	SA(s)c	657	6.5 <sup>o</sup>	25 <sup>o</sup>	9.0		1	9.95	0.25	-20.07	2002ap, 2003gd
10314		1058	02193	SA(rs)c	518	58.5	90.4	9.86	± 0.61	1	11.82	0.22	-18.37	1969L, 2007gr
10488		1097		SB(s)b	1271	55.0	138.2	14.2	± 2.6	1	10.23	0.10	-20.63	1992bd, 1999eu, 2003B
10496		1087	02245	SAB(rs)c	1517	54.2	12	14.4	± 1.8	1	11.46	0.12	-19.46	1995V
14814		1559		SB(s)cd	1304	60.2	62.8	12.6	± 2.5	1	11.00	0.11	-19.61	1984J, 1986L, 2009ib
15821		1637		SAB(rs)c	717	31.1	16.3	9.77	± 1.82	1	11.47	0.15	-18.63	1999em
17223		— LMC —		SB(s)m	278	35.3	170	0.050	± 0.002	m	0.91	0.27	-17.86	1987A
17609		2082		SB(r)b	1184	26.2	—	13.1	± 1.8	1	12.62	0.21	-18.18	1992ba
21396		2403	03918	SAB(s)cd	131	61.3	126	3.16	± 0.16	c,d,k,l	8.93	0.14	-18.74	2004dj
27978		2997		SA(s)c	1088	54.3	96.6	11.3	± 0.8	1	10.06	0.39	-20.59	2003gj, 2008eh
28630	81	3031	05318	SA(s)ab	-34	62.7	157	3.65	± 0.18	a,d,e,k,l	7.89	0.29	-20.18	1993J
30087		3184	05557	SAB(rs)cd	592	14.4	135	13.0		1	10.36	0.06	-20.27	1921B, 1937F, 1999gi
30560		3239	05637	IB(s)m pec	753	46.8	—	10.0		1	11.73	0.12	-18.39	2012A
32007	95	3351	05850	SB(r)b	778	54.6	9.9	10.0	± 1.0	c,d,h,l	10.53	0.10	-19.76	2012aw
40396		4369	07489	(R)SA(rs)a	1045	18.9	—	11.2	± 1.1	1	12.33	0.09	-18.01	2005kl
41399		4487		SAB(rs)cd	1034	58.2	74.2	11.0	± 0.8	1	11.69	0.08	-18.59	2009N
42575		4618	07853	SB(rs)jm	544	57.6	40.2	9.20	± 0.57	1	11.22	0.08	-18.67	1985F
43238		4691		(R)SB0/a(s) pec	1110	38.8	28.0	12		1	11.66	0.10	-18.84	1997X
47404	51a	5194	08493	SA(s)bc pec	463	32.6	163.0	8.39	± 0.84	b,l	8.96	0.13	-20.79	1994I, 2005cs, 2011dh
48082	83	5236		SAB(s)c	513	14.1	45 <sup>o</sup>	4.92	± 0.25	g,l	8.20	0.24	-20.29	1923A, 1968L, 1983N
50063	101	5457	08981	SAB(rc)cd	241	16	—	6.96	± 0.35	b,d,h,l	8.31	0.03	-20.99	1909A, 1951H, 1970G
50779		— Circinus —		SA(s)b?	434	64.3	36.1	4.21	± 0.78	1	12.10	2.00	-18.02	1996cr
54849		5921	09824	SB(r)bc	1480	49.5	140.0	14.0	± 3.2	1	11.49	0.15	-19.39	2001X
62836		6744		SAB(r)bc	841	53.5	15.4	11.6	± 0.9	1	9.61	0.16	-21.34	2005at
65001		6946	11597	SAB(rs)cd	40	18.3	—	7.0		1	9.61	1.24	-20.86	1917A, 1948B, 1968D 1980K, 2002hh, 2004et
68941		7292	12048	IBm	986	54.5	101.0	12.9	± 1.0	1	13.03	0.23	-17.75	1964H
69470			12160	Scd?	1555	38.1	14.8	14.4	± 3.0	1	14.85	2.04	-17.98	1995X
70096		7424		SAB(rs)cd	939	59	—	7.94	± 0.77	1	10.96	0.04	-18.56	2001ig
73049		7793		SA(s)d	227	53.7 <sup>n</sup>	99.3 <sup>n</sup>	3.61	± 0.18	1	9.63	0.07	-18.42	2008bk
02052		150		SB(rs)b?	1584	<b>66.9</b>	—	14.9	± 2.2	1	12.00	0.05	-18.92	1990K
09031		891	01831	SA(s)b? edge	528	<b>90</b>	—	9.91	± 0.5	c,e,l	10.81	0.24	-19.47	1986J
10329		1073	02210	SB(rs)c	1208	52.3	—	12.3	± 1.7	1	11.47	0.14	-19.12	1962L
12286		1313		SB(s)d	470	34.8	—	4.25	± 0.21	f,l	9.20	0.40	-19.25	1962M
22338		— ESO 209-G009 —		SB(s)cd? edge	1119	<b>90</b>	—	13.4	± 1.0	1	12.68	0.94	-18.89	2005ae
26512		2841	04966	SA(r)b?	638	<b>65.2</b>	—	14.1	± 1.4	1	10.09	0.06	-20.71	1972R
28655	82	3034	05322	I0 edge	203	<b>76.9</b>	—	3.52	± 0.18	k,l	9.30	0.58	-18.91	2004am, 2008iz
30197		3198	05572	SB(rs)c	663	<b>77.8</b>	—	13.8	± 1.4	1	10.87	0.05	-19.87	1966J
33408		3510	06126	SB(s)m edge	713	<b>78.1</b>	—	14.7	± 1.7	1	14.30	0.11	-16.65	1996cb
34030	108	3556	06225	SB(s)cd edge	699	<b>67.5</b>	—	9.55	± 1.26	1	10.69	0.06	-19.27	1969B
34695	66	3627	06346	SAB(s)b	727	<b>67.5</b>	—	8.28	± 0.41	c,d,l	9.65	0.12	-20.48	1973R, 2009hd
39225		4214	07278	IAB(s)m	291	43.7	—	2.87	± 0.14	k,l	10.24	0.08	-17.25	1954A
39600	106	4258	07353	SAB(s)bc	448	<b>68.3</b>	—	7.61	± 0.38	c,e,i,j,l	9.10	0.06	-20.28	1981K
41333		4490	07651	SB(s)d pec	565	<b>79</b>	—	9.20	± 0.57	1	10.22	0.08	-19.68	1982F, 2008ax
42002		4559	07766	SAB(rc)cd	807	64.8	—	8.67	± 0.57	1	10.46	0.06	-19.29	1941A
43451		4725	07989	SAB(r)sb pec	1206	45.4	—	12.4	± 1.2	1	10.11	0.04	-20.40	1940B
45279		4945		SB(s)cd? edge	563	<b>90</b>	—	3.36	± 0.17	1	9.30	0.64	-19.25	2005af, 2011ja
51106		5530		SA(rs)bc	1194	<b>66.5</b>	—	11.8	± 2.2	1	11.78	0.42	-19.00	2007it
67671			11861	SABdm	1481	<b>75</b>	—	14.4	± 3.0	1	14.20	2.19	-18.78	1995ag, 1997db
68618		— IC 5201 —		SB(rs)cd	915	<b>66.7</b>	—	9.20	± 1.71	1	11.30	0.04	-18.56	1978G
69327		7331	12113	SA(s)b	816	<b>70</b>	—	14.7	± 1.5	1	10.35	0.33	-20.82	1959D
71866		7713		SB(r)d?	692	<b>65.9</b>	—	9.95	± 2.07	1	11.51	0.06	-18.54	1982L

a: Ciardullo, Jacoby & Tonry (1993); b: Feldmeier et al. (1997); c: Ciardullo et al. (2002); d: Freedman et al. (2001); e: Tonry et al. (2001); f: Méndez et al. (2002); g: Thim et al. (2003); h: Sakai et al. (2004); i: Macri et al. (2006); j: Mager, Madore & Freedman (2008); k: Dalcanton et al. (2009); l: Tully et al. (2009); m: Schaefer (2008); n: Carignan & Puche (1990); o: Kamphuis & Briggs (1992) p: Danver (1942)

In addition, high spatial resolution H $\alpha$  imaging of several ccSNe host galaxies has been included in our extragalactic Wolf–Rayet surveys. These comprise VLT/FORS2 imaging of M83 (Hadfield et al. 2005) plus unpublished VLT/FORS1 imaging of M74 [from 380.D-0282(A), PI: P. Crowther] and NGC 6744 [081.B-0289(C), PI P. Crowther] and unpublished Gemini-N GMOS H $\alpha$  imaging of NGC 6946 (GN-2009B-Q-4, PI J. Bibby). The relatively small field

of view of these instruments excluded the investigation of some ccSNe environments in these galaxies from our VLT or Gemini imaging, although (non-calibrated) archival VLT/FORS1 imaging is available for the SN 2008bk in NGC 7793 [067.D-0006(A), PI: W. Gieren].

Flux calibration was necessary in these cases. The LMC Nikon survey camera image was calibrated against PLC data sets for 30

**Table 5.** Source of ground-based H $\alpha$  and continuum imaging used in this study.

Tel ID	Telescope	Instrument	CCD scale (arcsec/pix)	FWHM (arcsec)	— H $\alpha$ —		Continuum	Reference
					$\lambda_c$ (Å)	FWHM (Å)		
a1	Nikon Survey Camera	2K CCD	12.0	30	6570	15	HaC (6676, 55)	Murphy & Bessell (2000)
a2	Parking Lot Camera	800×800	36.9	80	6571	14	R	Kennicutt et al. (1995)
b	KPNO 0.6 m Schmidt	Tek 2K CCD	2.03	4.4	6573	67	R	Hoopes, Walterbos & Bothun (2001)
c	CTIO 0.9 m	Tek 2K CCD	0.792	~3.0	6563	75	R	Kennicutt et al. (2008)
d1	JKT 1.0 m	CCD	0.241	1.5–2	6594	44	R	Knapen et al. (2004)
d2			0.331	1.5–3	6594	44	R	James et al. (2004)
e1	CTIO 1.5 m	CCD	0.434	1.0	6568	30	R	Meurer et al. (2006)
e2				1.2	6568	20	R	Kennicutt et al. (2003)
f	Danish 1.54 m	DFOSC	0.400	1.8	6565	114	R	Larsen & Richtler (1999)
g	VATT 1.8 m	CCD	0.400	~1.8	6580	69	R	Kennicutt et al. (2008)
h	KPNO 2.1 m	CFIM	0.305	1.0	6573	67	R	Kennicutt et al. (2003)
i	Bok 2.3 m	CCD21	0.432	~1.5	6575	69	R	Kennicutt et al. (2008)
j1 <sup>1</sup>	VLT 8.0 m	FORS1+2	0.126	0.8	6563	61	HaC (6665, 65)	Hadfield et al. (2005)
j2 <sup>2</sup>			0.200	0.8	6563	61	V	
k <sup>3</sup>	Gemini-N 8.1 m	GMOS	0.145	0.6	6560	70	HaC (6620, 60)	
l1	INT 2.5 m	WFC	0.333	1.8	6568	95	R	Anderson & James (2008)
l2				1–2	6568	95	HaC (6657, 79), r	
m	LT 2.0 m	RATCam	0.278	1.2	6557	100	r'	Anderson & James (2008)
n	CFHT 3.6 m	CFH12K	0.206	0.9	6584	96	R	Crockett et al. (2007)

1: 067.D-0006(A), 069.B-0125(A), 380.D-0282(A), 081.B-0289(C); 2: 075.D-0213(A); 3: GN-2009B-Q-4

Doradus (Kennicutt et al. 1995). The Danish 1.54 m data sets of Larsen & Richtler (1999) were calibrated with respect to five galaxies in common with 11HUGS (NGC 300, NGC 1313, M83, NGC 6946, NGC 7793). VLT/FORS1+2 and Gemini-G GMOS images were calibrated against imaging of spectrophotometric standard stars (LTT 4816, LTT 1020, BD+28 4211).

Finally, where necessary (e.g. H $\alpha$ GS), astrometric calibration was performed using the Starlink *Gaia* package<sup>10</sup> using the USNO-A2 catalogue, with typical RMS of <1 pix, corresponding to <0.5 arcsec in the majority of instances.

For this sample, eight (19 per cent) of the ccSNe originate from early-type spirals (S0/a/b), 31 (76 per cent) from late-type spirals (Sc/d/m) and two (5 per cent) from irregulars (Im). 25 (61 per cent) ccSNe are from high-luminosity ( $M_B < -19$  mag) hosts, with 16 (39 per cent) from low-luminosity galaxies, with a similar fraction of Type II and Type Ib/c ccSNe from dwarf hosts.

Table 6 presents star formation rates (SFR) and star formation intensities for all host galaxies, excluding those lacking calibrated H $\alpha$  imaging (NGC 2082, 4369, 4691, UGC 12160). H $\alpha$  fluxes are adjusted for the contribution of [N II]  $\lambda\lambda$ 6548–6583 preferentially from integrated spectrophotometry (e.g. Moustakas & Kennicutt 2006) or the Lee et al. (2009b)  $M_B$ -calibration. Similarly, extinction corrections,  $A_{H\alpha}$ , are preferentially obtained from measured integrated nebular H $\alpha$ /H $\beta$  ratios (e.g. Moustakas & Kennicutt 2006, via equation 4 from Lee et al. 2009b), or are the sum of (measured) foreground and (estimated) internal extinctions. Foreground extinctions are from Schlafly & Finkbeiner (2011, recalibration of Schlegel, Finkbeiner & Davis 1998), for which we assume  $A_{H\alpha} = 0.62 A_B$ , while internal extinctions are estimated from a scaling relation between extinction and  $M_B$  (Lee et al. 2009b). In the case of Circinus, an extinction of  $A_B = 2.0$  mag was adopted (Freeman et al. 1977) owing to its low galactic latitude.

Integrated fluxes largely confirm previous results (e.g. Lee et al. 2009b), aside from differences in distances and the source of fluxes.

One notable exception is NGC 6744, for which the newly calibrated Larsen & Richtler (1999) data sets reveal a lower limit of  $4.7 \times 10^{-12}$  erg s<sup>-1</sup> cm<sup>-2</sup> (6.4 arcmin radius) to the H $\alpha$ + [N II] flux, significantly higher than  $2.0 \times 10^{-12}$  erg s<sup>-1</sup> cm<sup>-2</sup> from Ryder & Dopita (1993), as reported in Kennicutt et al. (2008). A net flux of  $1.2 \times 10^{-12}$  erg s<sup>-1</sup> cm<sup>-2</sup> within the central region (3.5 arcmin radius) from Larsen & Richtler (1999) matches that from the calibrated VLT/FORS1 data set to within 2 per cent. Uncertainties for hosts in which fluxes, [N II]/H $\alpha$  and reddenings have been measured, such as M74, are typically  $\pm 20$  per cent, whereas cases for which calibrations have been adopted for [N II]/H $\alpha$  (factor of 2) and  $A_{H\alpha}$  ( $\pm 50$  per cent), such as NGC 337A, are typically  $\pm 40$  per cent.

Star formation intensities are uniformly based upon  $R_{25}$ , although the intensity is also calculated for the LMC from its  $V$ -band scalelength,  $R_D$  (Hunter & Elmegreen 2004), following Bothun & Thompson (1988).

### 3.3 Calculation of H $\alpha$ luminosities

We have calculated H $\alpha$  luminosities of H II regions in close proximity to the ccSNe location in the following way. Fluxes were measured using apertures no smaller than the image FWHM. Aside from the LMC Nikon Survey Camera and CTIO 1.5 m/Cass Focus CCD imaging, H $\alpha$  filters include the contribution of [N II]  $\lambda\lambda$ 6548–84. To adjust for this contribution, we either selected the [N II]/H $\alpha$  ratio measured from spectrophotometry of their host galaxies or estimated the ratio from an empirical scaling relation between [N II]/H $\alpha$  and the absolute  $B$ -band magnitude  $M_B$  (Kennicutt et al. 2008), as above for global SFR. Of course, this adds an additional uncertainty, namely the radial metallicity gradient. By way of example, Bresolin et al. (2004) measured  $0.31 \leq [\text{N II}]/\text{H}\alpha \leq 0.64$  for 10 H II regions spanning the full radial extent of the disc of M51a. Here, we adopt [N II]/H $\alpha$  = 0.59 (Moustakas & Kennicutt 2006), such that H $\alpha$  luminosities should be underestimated by, at most,  $\sim 20$  per cent in the outer disc where metallicities are lower than average. However, no correction is attempted due to the azimuthal variation in metallicity,

<sup>10</sup> <http://star-www.dur.ac.uk/pdraper/gaia/gaia.html>

**Table 6.** Integrated H $\alpha$  + [N II] fluxes (H $\alpha$  in italics) of host galaxies of ccSNe used in this study, from which SFR and star formation intensities ( $\Sigma$ ) are obtained. Galaxy radii are from RC3 or HyperLeda ( $R_{25}$ ), or Bothun & Thompson (1998,  $R_D$ ). Uncertainties, where known, are indicated, while the [N II]/H $\alpha$  calibration from Lee et al. (2009b) is reliable to a factor of 2, and the  $A_{H\alpha}$  calibration is robust to  $\pm 50$  per cent, such that global H $\alpha$  luminosities (SFR and  $\Sigma$ ) should be reliable to between  $\pm 20$  per cent (direct measurements of [N II]/H $\alpha$  and  $A_{H\alpha}$ ) and  $\pm 40$  per cent (calibrations).

PGC	Alias	$d$ (Mpc)	$\log F(\text{H}\alpha + [\text{N II}])$ (erg s $^{-1}$ cm $^{-2}$ )	Ref	[N II]/H $\alpha$	$A_{H\alpha}$ (mag)	Ref	$L(\text{H}\alpha)$ (erg s $^{-1}$ )	SFR (M $_{\odot}$ yr $^{-1}$ )	$R_{25}$ ( $R_D$ ) (arcmin)	$R_{25}$ ( $R_D$ ) (kpc)	$\Sigma_{R_{25}}$ ( $\Sigma_{R_D}$ ) (M $_{\odot}$ yr $^{-1}$ kpc $^{-2}$ )
03671	NGC 337A	11.4	$-11.73 \pm 0.10$	6, 9 (d1)	0.16	0.71	9( $M_B$ )	$4.8 \times 10^{40}$	0.38	2.9	9.7	$1.3 \times 10^{-3}$
05974	M74	9.0	$-10.84 \pm 0.04$	1	$0.35 \pm 0.05$	$0.30 \pm 0.18$	3	$1.4 \times 10^{41}$	1.1	5.2	13.7	$1.8 \times 10^{-3}$
10314	NGC 1058	9.86	$-10.63 \pm 0.05$	1	$0.48 \pm 0.05$	$0.69 \pm 0.22$	5	$3.5 \times 10^{40}$	0.27	1.5	4.3	$4.7 \times 10^{-3}$
10488	NGC 1097	14.2	$-10.95$	3	0.46	$1.50 \pm 0.08$	9( $M_B$ ),3	$7.3 \times 10^{41}$	5.8	4.7	19.2	$5.0 \times 10^{-3}$
10496	NGC 1087	14.4	$-11.30 \pm 0.04$	2	$0.40 \pm 0.03$	$0.75 \pm 0.20$	5	$1.8 \times 10^{41}$	1.4	1.9	7.8	$7.4 \times 10^{-3}$
14814	NGC 1559	12.6	$-10.81 \pm 0.10$	9 (j2)	0.31	0.86	9( $M_B$ )	$4.9 \times 10^{41}$	3.9	1.7	6.3	$3.1 \times 10^{-2}$
15821	NGC 1637	9.77	$-11.59 \pm 0.07$	4, 9 (e1)	0.85	0.69	8, 9( $M_B$ )	$3.0 \times 10^{40}$	0.24	2.0	5.6	$2.4 \times 10^{-3}$
17223	LMC	0.05	$-6.96 \pm 0.05$	1	0.15	0.64	9( $M_B$ )	$5.0 \times 10^{40}$	0.40	323 (103)	4.7 (1.5)	$5.8 \times 10^{-3}$ ( $5.6 \times 10^{-2}$ )
21396	NGC 2403	3.16	$-10.25 \pm 0.04$	1	$0.22 \pm 0.04$	$0.45 \pm 0.20$	3	$8.5 \times 10^{40}$	0.67	10.9	10.1	$2.1 \times 10^{-3}$
27978	NGC 2997	11.3	$-10.80 \pm 0.10$	7, 9 (f)	0.46	1.25	9( $M_B$ )	$5.1 \times 10^{41}$	4.1	4.5	14.6	$6.1 \times 10^{-3}$
28630	M81	3.65	$-10.31 \pm 0.02$	1	$0.55 \pm 0.08$	$0.15^{+0.30}_{-0.15}$	3	$5.8 \times 10^{40}$	0.46	13.5	14.2	$7.1 \times 10^{-4}$
30087	NGC 3184	13.0	$-11.12 \pm 0.05$	3	$0.52 \pm 0.05$	$0.63 \pm 0.18$	3	$1.8 \times 10^{41}$	1.4	3.7	14.0	$3.1 \times 10^{-3}$
30560	NGC 3239	10.0	$-11.32 \pm 0.03$	1	$0.09 \pm 0.01$	$0.30 \pm 0.21$	5	$6.9 \times 10^{40}$	0.55	2.5	7.3	$3.3 \times 10^{-3}$
32007	M95	10.0	$-11.24 \pm 0.08$	1	$0.66 \pm 0.03$	$0.73 \pm 0.17$	3	$8.1 \times 10^{40}$	0.64	3.7	10.7	$1.8 \times 10^{-3}$
41399	NGC 4487	11.0	$-11.93 \pm 0.10$	6, 9 (d1)	0.21	0.65	9( $M_B$ )	$2.9 \times 10^{40}$	0.23	2.1	6.7	$1.7 \times 10^{-3}$
42575	NGC 4618	9.2	$-11.36 \pm 0.04$	1	$0.28 \pm 0.03$	$0.13^{+0.21}_{-0.13}$	5	$3.9 \times 10^{40}$	0.31	2.1	5.6	$3.2 \times 10^{-3}$
47404	M51a	8.39	$-10.42 \pm 0.08$	1	$0.59 \pm 0.01$	$1.05 \pm 0.21$	5	$5.3 \times 10^{41}$	4.2	5.6	13.6	$7.1 \times 10^{-3}$
48082	M83	4.92	$-10.00 \pm 0.04$	1	0.40	1.08	9( $M_B$ )	$5.6 \times 10^{41}$	4.4	6.4	9.2	$1.7 \times 10^{-2}$
50063	M101	6.96	$-10.22 \pm 0.13$	1	0.54	1.10	9( $M_B$ )	$6.3 \times 10^{41}$	5.0	14.4	29.1	$1.9 \times 10^{-3}$
50779	Circinus	4.21	$-11.19 \pm 0.06$	1	0.16	1.74	9( $M_B$ )	$5.8 \times 10^{40}$	0.46	3.5	4.2	$8.2 \times 10^{-3}$
54849	NGC 5921	14.0	$-11.63 \pm 0.05$	2	0.28	0.83	9( $M_B$ )	$9.3 \times 10^{40}$	0.73	2.5	9.9	$2.4 \times 10^{-3}$
62836	NGC 6744	11.6	$-11.33^a$	7, 9 (f)	0.61	1.28	9( $M_B$ )	$1.5 \times 10^{42a}$	12.0 $^a$	10.0	33.6	$3.4 \times 10^{-3a}$
65001	NGC 6946	7.0	$-10.42 \pm 0.06$	3	$0.45 \pm 0.09$	$0.45 \pm 0.30$	3	$2.3 \times 10^{41}$	1.8	5.7	11.7	$4.3 \times 10^{-3}$
68941	NGC 7292	12.9	$-11.78 \pm 0.04$	2	0.15	0.60	9 ( $M_B$ )	$5.0 \times 10^{40}$	0.39	1.1	4.0	$7.8 \times 10^{-3}$
70096	NGC 7424	7.94	$-11.28 \pm 0.07$	4, 9 (e1)	0.20	0.62	9( $M_B$ )	$5.7 \times 10^{40}$	0.45	4.8	11.0	$1.2 \times 10^{-3}$
73049	NGC 7793	3.61	$-10.60 \pm 0.08$	3	$0.31 \pm 0.07$	$0.67 \pm 0.16$	3	$5.5 \times 10^{40}$	0.44	4.7	4.9	$5.8 \times 10^{-3}$

1: Kennicutt et al. (2008); 2: James et al. (2004); 3: Kennicutt et al. (2009); 4: Meurer et al. (2006); 5: Moustakas & Kennicutt (2006); 6: Knapen et al. (2004); 7: Larsen & Richtler (1999); 8: Kennicutt & Kent (1983); 9: this work (note)

$^a$ Lower limit using aperture of radius 6.4 arcmin (0.64  $R_{25}$ ).

as shown from integral field spectroscopy of M74 by Sánchez et al. (2011, their fig. 17).

Corrected H $\alpha$  fluxes were converted into intensities, using the method set out above for global SFR. Once again, we neglect spatial variations of internal extinctions. For example, a global average of  $A_{H\alpha} = 1.05$  mag is adopted for M51a (Moustakas & Kennicutt 2006), whereas Bresolin et al. (2004) obtained  $0.09 \leq A_{H\alpha} \leq 1.05$  mag for 10 H II regions distributed throughout its disc.<sup>11</sup> For M51a, the luminosity of individual H II regions may be overestimated by up to a factor of 2.5. Once again, no radial correction is attempted owing to the clumpy nature of dust attenuation, as shown in integral field spectroscopy of M74 by Sánchez et al. (2011, their fig. 11).

Overall, our adoption of global [N II]/H $\alpha$  and  $A_{H\alpha}$  values should have a negligible effect for the majority of sources, such that the 20–40 per cent uncertainties quoted above will apply to individual H II regions. However, H $\alpha$  luminosities of regions far from large H II complexes – typically those at large galactocentric radii – may be overestimated by up to a factor of 2 ([N II]/H $\alpha$  and  $A_{H\alpha}$  corrections act in opposite senses). The average galactocentric distance is  $R_{SN}/R_{25} = 0.47$  ( $\sigma = 0.30$ ), although H $\alpha$  luminosities of nebulae located in the extreme outer discs of their hosts may be overestimated (e.g. SN 1980K, SN 2001ig, SN 2002ap, SN 2004et). Nevertheless, such adjustments would not affect our main conclusions.

<sup>11</sup> We have converted the  $c(H\beta)$  values from Bresolin et al. (2004) to  $A_{H\alpha}$  via  $E(B - V) \sim 0.7 c(H\beta)$  and  $A_{H\alpha} \sim 2.5 E(B - V)$ .

### 3.4 Results

Following van Dyk (1992), a ccSNe is considered to be associated with an H II region if it is offset by an amount less than or equal to the radius of the H II region. For example, SN 1923A lies 4 arcsec from an H II region whose radius is  $\sim 4$  arcsec, while SN 1964H lies 5 arcsec from an H II region, whose radius is 2 arcsec. Therefore, the former is considered to be associated with an H II region while the latter is not. More detailed notes relating to individual ccSNe are provided in Appendix A.

Tables 2–3 present basic properties of individual Type Ib/c and Type II ccSNe, respectively, including the radius and H $\alpha$  flux/luminosity of the nearest H II region. Overall, approximately half (18 of the 39) of our sample of ccSNe are associated with H II regions. Of these, the mean H $\alpha$  luminosity is  $3 \times 10^{38}$  erg s $^{-1}$ , excluding SN 1970G which lies at the periphery of the supergiant H II region NGC 5455 within M101. If we now separate these ccSNe into their main types, a much higher fraction of Type Ib/c ccSNe (7 out of 10), namely  $70 \pm 26$  per cent, are associated with nebular emission than Type II ccSNe (11 out of 29), for which the fraction is  $38 \pm 11$  per cent. This is qualitatively in agreement with the ground-based studies of Anderson & James (2008) and Anderson et al. (2012).

However, recall the lack of an association between H II regions and nearby ( $cz < 2000$  km s $^{-1}$ ) ccSNe (Smartt et al. 2009) discovered between 1998 and 2008.5 observed at high spatial resolution (Crockett 2009; Smartt, private communication). Only four Type II ccSNe are in common between this study and the subset of ccSNe

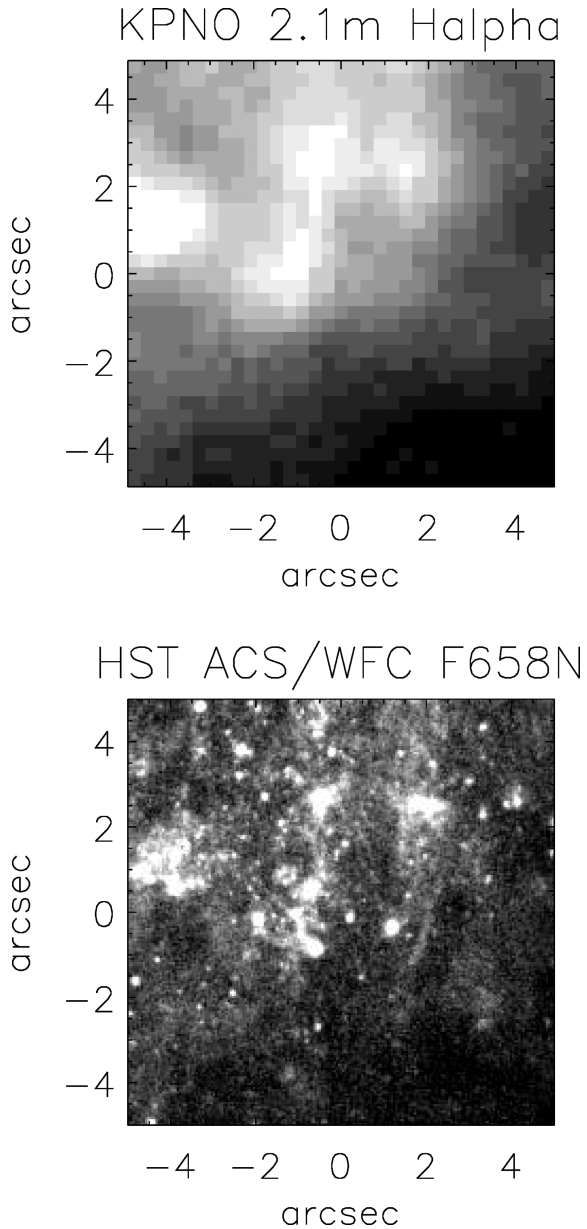


**Figure 2.** Top:  $10 \times 10$  arcsec<sup>2</sup> KPNO 2.1 m H $\alpha$  image (from Kennicutt et al. 2003) showing the environment of SN 2005cs in M51a, corresponding to  $400 \times 400$  pc at a distance of 8.39 Mpc; bottom: multidrizzled *HST* ACS/WFC F658N image from GO 10452 (PI: S. Beckwith; see discussion in Li et al. 2006). North is up and east is to the left.

from Smartt et al. (2009) that have been observed with *HST*. Of these, the ground-based study reveals consistent results, except for SN 2005cs (II-P). Fig. 2 shows that SN 2005cs appears to be associated with nebular emission from ground-based KPNO 2.1 m imaging, yet *HST* ACS/WFC imaging reveals that it is offset by  $\sim 1$  arcsec (40 pc at 8.4 Mpc), as discussed by Li et al. (2006).

Turning to Ib/c ccSNe, only three are in common between this study and Crockett (2009). Broadly consistent results are obtained, although SN 2007gr (Ic) merits discussion, since it is the only Ib/c associated with a star-forming region at the spatial resolution of *HST*. SN 2007gr is formally associated with H $\alpha$  emission on the basis of our ground-based imaging (Fig. A32), whereas Crockett et al. (2008) indicate a small offset from H $\alpha$  emission (from INT/WFC).

More recent *HST* WFPC2/F675W and WFC3/F625W suggest that faint nebulosity is spatially coincident with the SN position.

In Table 7, we provide a summary of these results, together with previous related studies. Despite the low number statistics, our results have the advantage over previous ground-based studies owing to smaller positional uncertainties with respect to van Dyk et al. (1996) and significantly smaller average distances than Anderson et al. (2012). For a nominal ground-based imaging quality of FWHM  $\sim 1.5$  Å, the typical spatial resolution achieved is 125 pc (van Dyk et al. 1996), 260 pc (Anderson et al. 2012) and 70 pc in this work. A characteristic scale of  $\sim 10$  pc – an order of magnitude higher – is achieved from the *HST*-selected sample of Smartt et al. (2009) and Crockett (2009). This is likely the origin of the very different statistics with respect to the ground-based studies. We shall return to the issue of spatial resolution in Section 5.

## 4 IMPLICATIONS FOR PROGENITOR MASSES OF CCSNE

### 4.1 Core-collapse SN environments

We now attempt to combine our results with the earlier discussion to place constraints upon ccSNe progenitors, recognizing that this approach is inferior to those methods involving photometric detection of immediate ccSNe progenitors (e.g. Smartt et al. 2009).

We have examined the environment of each ccSNe and assign each case to one of the five classes set out in Section 2. For our previous examples, SN 1923A narrowly lies within the radius of a luminous H II region (Fig. A1), so it is assigned to Class 5, whereas SN 1964H lies far from nebular emission (Fig. A2), so it is assigned to Class 2 since it is not coincident with a bright star cluster.

Unsurprisingly, owing to the poor spatial resolution and sensitivity of the ground-based imaging, only one of the ccSNe, SN 2004dj (II-P), was assigned to Class 1, i.e. nebular emission absent but (young) cluster detected, as shown in Fig. A27. A massive progenitor ( $>20 M_{\odot}$ ) might be expected for SN 2004dj, although detailed studies of the cluster indicate a lower progenitor mass  $<20 M_{\odot}$  (Vinkó et al. 2006, 2009). As discussed above for the case of SN 2005cs (Fig. 2), more ccSNe from our sample would have been included in this category on the basis of *HST* imaging (e.g. SN 2009ib).

Half of Type II ccSNe (15 from 29) were assigned to Class 2, i.e. ccSNe lacking nebular emission, an associated (bright) cluster or a nearby giant H II region. The progenitor masses of such are expected to be  $<20 M_{\odot}$ , in accord with Smartt et al. (2009) since the majority of these H-rich ccSNe either have unknown subclass or are Type II-P – exceptions are Type IIb ccSNe SN 1993J (Fig. A12) and SN 2011dh (Fig. A37).

Two H-deficient ccSNe also fall in this category (SN 2002ap, SN 2003jg), of which SN 2002ap represents an archetypal case (Fig. A22). The inclusion of Type Ic ccSNe in this category favours an interacting binary scenario over a single star progenitor for these cases, as discussed by Crockett et al. (2007) for SN 2002ap. Indeed, Mazzali et al. (2002, 2007) proposed a binary scenario for SN 2002ap involving a progenitor with  $15\text{--}25 M_{\odot}$ . The case of SN 2003jg is marginal since it lies 2 arcsec away (140 pc deprojected) from an H II region, whose radius is 1.5 arcsec on the basis of ground-based Danish 1.5 m imaging (Fig. A26) such that it narrowly fails to meet our threshold for association.

From our sample, we identify three potential runaways from nearby giant H II regions (Class 3), namely SN 1986L (II-L), SN 1997X (Ib) and SN 2001X (II-P), of which the former serves as

**Table 7.** Summary of this work and related studies, indicating sample size,  $N_{\text{SNe}}$ , mean distances,  $\bar{d}$ , the number of ccSNe associated with H II regions,  $N_{\text{H II}}$  or the normalized cumulative rank (NCR) pixel (see James & Anderson 2006). Distances are obtained from individual SN hosts, drawn preferentially from the EDD ( $\leq 3000 \text{ km s}^{-1}$ ; Tully et al. 2009) or otherwise NASA Extragalactic Database.

SN type	van Dyk et al. (1996)			Anderson et al. (2012)			Smartt (priv. comm.)			This work		
	$N_{\text{SNe}}$	$\bar{d}$ (Mpc)	$N_{\text{H II}}/N_{\text{SNe}}$	$N_{\text{SNe}}$	$\bar{d}$ (Mpc)	$\overline{\text{NCR}}^a$	$N_{\text{SNe}}$	$\bar{d}$ (Mpc)	$N_{\text{H II}}$	$N_{\text{SNe}}$	$\bar{d}$ (Mpc)	$N_{\text{H II}}/n_{\text{SNe}}$
II	32	16.2	$72 \pm 10$ per cent	163.5	32	$0.25 \pm 0.02$	17	14.6	0	29	8.7	$38 \pm 11$ per cent
Ib				39.5	40	$0.32 \pm 0.04$						
Ic	17	17.7	$68 \pm 12$ per cent	52	42	$0.47 \pm 0.04$	9	19.3	1	10	9.9	$70 \pm 26$ per cent

<sup>a</sup>NCR = 0 if the ccSN site is not associated with any H $\alpha$  emission and NCR = 1 if it is associated with the brightest H $\alpha$  emission in its host.

a useful example (Fig. A9). Here, we consider possible runaways if they lie at deprojected distances of up to 0.4 kpc from luminous H II regions ( $L(\text{H}\alpha) \geq 10^{38} \text{ erg s}^{-1}$ ). If this were so, we are unable to assign progenitor masses, although high runaway masses are believed to be favoured (Fujii & Portegies Zwart 2011). Of course, the presence of a nearby giant H II region does not require a high-mass cluster that is sufficiently dense for runaways via dynamical interactions during the cluster formation. In addition, the close proximity of a giant H II region to the ccSNe does not necessarily imply the progenitor originated from this region (Class 2 is also likely).

Turning to ccSNe which are associated with H II regions, we find six cases matching Class 4, involving a relatively faint H II region in close proximity to the ccSN. Of these, every H II region is spatially extended, namely SN 1983N (Ib), SN 1987A (IIpec), SN 2001ig (Iib), SN 2005at (Ic), SN 2005cs (II-P) and SN 2012A (II-P), indicating a lower limit to the progenitor mass of 12 (20)  $M_{\odot}$  for a duty cycle of 20 (10) Myr. We cannot exclude the possibility of higher mass progenitors since the H II regions identified as extended from ground-based imaging may involve multiple compact H II regions in some instances. Still, close binary (accretion or merger) predictions favour a mass of  $\sim 15 M_{\odot}$  for the progenitor of SN 1987A (Podsiadlowski 1992). Panagia et al. (2000) discuss a loose  $12 \pm 2$  Myr cluster likely to be associated with the progenitor of SN 1987A, although this would not be detected in ground-based imaging at the typical distance of other ccSNe in our sample.

The spatial resolution of ground-based observations certainly limits the potential association with H II regions (recall Table 7). Fig. 2 contrasts (non-Adaptive Optics) ground-based and space-based H $\alpha$  imaging of the immediate environment of SN 2005cs. *HST* imaging reveals several compact H II regions that are in close proximity to the ccSNe, albeit none spatially coincident with it, although, in addition, bright H II regions are often in close proximity to the SN site, such that a runaway status cannot be excluded either (e.g. SN 1983N, Fig. A7).

Finally, 12 of the 39 ccSNe are associated with giant H II regions (Class 5), comprising  $50 \pm 22$  per cent (5/10) of the Type Ib/c SNe, though only  $24 \pm 9$  per cent (7/29) of the Type II ccSNe sample. Solely SN 1985F (Ib/c) is spatially coincident with a bright cluster (Fig. A8), while some others are found in complexes (e.g. SN 2007gr, Fig. A32). Age estimates for individual stellar populations within each region are not available, so we consider a characteristic duty cycle of (super)giant H II regions of 20 (10) Myr, from which lower progenitor mass limits of 12 (20)  $M_{\odot}$  are implied for the initial stellar generation, with higher limits for subsequent episodes of star formation. Unfortunately, no limit to the progenitor mass of SN 1968L (II-P) can be assigned since it lies within the nuclear starburst of M83 (Fig. A4).

Detailed studies based either on either pre-SN imaging (e.g. Aldering, Humphreys & Richmond 1994) or post-SN light curves (e.g. Chugai & Utrobin 2000) have been carried out in some cases.

For example, the former technique was used by Leonard et al. (2002) to obtain an upper limit of  $15_{-3}^{+5} M_{\odot}$  for the progenitor mass of SN 1999gi (II-P; see also Hendry 2006), while the latter approach enabled Iwamoto et al. (1994) to estimate a progenitor mass of  $\sim 15 M_{\odot}$  for SN 1994I (Ic). Therefore, a giant H II region duty cycle of 20 Myr is the most realistic case (recall also Section 2.3), which naturally provides only weak limits upon progenitor masses for these II-P, II n and Ib/c Types of ccSNe (e.g. Smartt 2009).

#### 4.2 Previous ccSNe environmental studies in context

We have attempted to constrain progenitor masses from the association between ccSNe and H II regions, or lack thereof. Overall, establishing progenitor masses in either case is challenging, given the *short* duration of the H II region phases for isolated, compact clusters and the *long* duration of the giant H II region phase for extended, star-forming complexes, which form the majority of the sample. SN 2004dj (II-P) ought to provide the strongest indirect (young) age constraint, since this is spatially coincident with a star cluster though not an H II region. However, direct analysis of its light curve suggests an old age/low mass (Vinkó et al. 2006, 2009). Therefore, ccSNe progenitor inferences from H II regions should be treated with caution, especially for high-inclination hosts and/or low spatial resolution observations.

How, then, should one interpret previous interpretations of the association between H II regions and ccSNe, or lack thereof? According to Anderson & James (2008), a progenitor mass sequence II  $\rightarrow$  Ib  $\rightarrow$  Ic was proposed, with H-rich ccSNe further subdivided into II n  $\rightarrow$  II-P  $\rightarrow$  II-L  $\rightarrow$  Iib by Anderson et al. (2012).

We concur with Anderson et al. that the higher frequency of Type Ibc with H II regions than Type II ccSNe arises from the relative lifetimes of their progenitors with respect to H II regions. However, we disagree with their implications since the H II regions detected at distances typical of their sample ( $\bar{d} = 35$  Mpc, Table 7) are extended, giant, multigeneration H II regions. Let us assume that Type II ccSNe result from progenitors with 8–20  $M_{\odot}$  (Smartt 2009) from the first stellar population. A duty cycle of  $\sim 20$  Myr would imply that 40 per cent of Type II progenitors with 12–20  $M_{\odot}$  are associated with H II regions, while 60 per cent of progenitors with 8–12  $M_{\odot}$  are not, based upon a standard Salpeter IMF slope for massive stars. Although approximate, such expectations agree well with the  $34 \pm 11$  per cent of Type II ccSNe that are associated with H II regions in our study.

To illustrate the restricted progenitor mass limits that can be achieved from this approach, the only case of a Type II n supernova in our present study is SN 1996cr. It has been proposed that these arise from massive luminous blue variables (Smith 2008), yet Anderson et al. (2012) claim that Type II n SN possesses the lowest mass progenitors of all massive stars. SN 1996cr is associated with a giant H II region, although is not coincident with a bright cluster, so

one can merely set a lower mass limit of  $12 M_{\odot}$  to the progenitor, with no robust upper limit, so one cannot argue against a high-mass progenitor on the basis of its immediate environment.

Of course, a higher fraction ( $70 \pm 26$  per cent) of Type Ib/c ccSNe are associated with H II regions. This suffers from small number statistics, but likely reflects the shorter lifetime of stars with  $\geq 12 M_{\odot}$ , the majority of which will be associated with an  $\sim 20$  Myr duty cycle of giant H II regions. In general, this fails to discriminate between most single star (Crowther 2007; Georgy et al. 2012), and close binary progenitor scenarios (Podsiadlowski et al. 1992; Yoon, Woosley & Langer 2010), aside from a higher mass threshold ( $\geq 12 M_{\odot}$ ?) for Ib/c than Type II ccSNe ( $\geq 8 M_{\odot}$ ). Still, for the two cases lacking any associated H II region or nearby giant H II region, SN 2002ap (Ic) and SN 2003jg (Ib/c), a close binary scenario is favoured.

## 5 DISCUSSION

### 5.1 Can local H II regions constrain ccSNe progenitor masses?

We have assessed the immediate nebular environment of ccSNe in nearby star-forming galaxies, and confirm the results from Anderson & James (2008) and Anderson et al. (2012) that Type Ib/c ccSNe are more likely to be associated with an H II region than Type II ccSNe. However, the typical H II regions identified in H $\alpha$  imaging from ground-based telescopes are extended, giant H II regions with long duty cycles. Indeed, the issue of differing duty cycles for compact, isolated H II regions versus extended, H II complexes is particularly relevant for late-type spirals and irregulars. Such hosts dominate the statistics of Anderson et al. (2012), for which large star-forming complexes – ionized by multiple generations of star clusters – are common (Kennicutt et al. 1989).

Nevertheless, firm limits upon the lifetime ( $\leq 4$  Myr) and mass ( $\geq 85 M_{\odot}$ ) of ccSNe progenitors would be possible if examples of isolated, classical H II regions could be identified. Resolving the specific location of the ccSNe within such a region is only realistic at much higher spatial resolution than typically achieved here, whether from space with *HST* or using Adaptive Optics with large ground-based telescopes (recall Fig. 2). From Table 7, ccSNe are rarely associated with compact H II regions, although this is unsurprising in view of the small numbers of very high mass stars within nearby star-forming galaxies.

Overall, we confirm previous findings by Anderson & James (2008) and Anderson et al. (2012) that the association between different SNe flavours and H II regions does vary between H-rich and H-poor ccSNe. Unfortunately, minimal implications for progenitor masses can be drawn which prevents discrimination between the single versus close binary progenitor scenarios proposed for Ib/c (and Iib) ccSNe (Anderson & James 2008). Our findings fail to support claims that the progenitors of IIc ccSNe possess relatively low masses (Anderson et al. 2012). In only a few cases does the lack of nebular emission provides limits upon progenitor masses, i.e. favouring the close binary scenario for two Type Ib/c ccSNe.

### 5.2 Core-collapse SNe beyond the local universe

Mindful of the spatial resolution issue, let us re-assess the Kelly et al. (2008) study of SNe locations, with respect to the continuum (*g*-band) light of their low-redshift ( $z < 0.06$ ) host galaxies. Kelly et al. revealed that Ic SNe are much more likely to be found in the brightest

regions of their hosts than Type II SNe, with intermediate properties for Type Ib SNe. Kelly et al. (2008) argued that if the brightest locations correspond to the largest star-forming regions, Type Ic SNe are restricted to the most massive stars, while Type Ib and especially Type II-P SNe are drawn from stars with more moderate masses.

The SN host sample of Kelly et al. (2008) is not expected to be significantly different from our present sample. From Table 6, star formation intensities from the present (spiral) hosts are uniformly high, with an average value of  $\Sigma_{R_{25}} = 5 \times 10^{-3} M_{\odot} \text{ yr}^{-1} \text{ kpc}^{-2}$ . This is more representative of ‘typical’ late-type (Scd) spirals, even for Sab hosts ( $\Sigma_{R_{25}} \sim 8 \times 10^{-3} M_{\odot} \text{ yr}^{-1} \text{ kpc}^{-2}$  for Circinus). For the irregular galaxies, comparisons with the reference galaxies are more difficult due to the lack of V-band scalelengths for NGC 3239 and NGC 7292. If intensities are typically an order of magnitude higher (on the basis of the LMC), these are intermediate between the extremes of the Small Magellanic Cloud (SMC) and NGC 1569.

Therefore, how should the difference between Type Ib/c and Type II ccSNe identified by Kelly et al. (2008) be explained? In the *g'* band, a star cluster will fade by 1 mag at young ages (5–10 Myr), with a further 1 mag dimming at intermediate ages (10 to  $\sim 60$  Myr), as shown in fig. 5 from Bik et al. (2003). Still, individual star clusters are not spatially resolved in ground-based imaging so it is more likely that the difference relates to the different frequencies of Type Ib/c and Type II ccSNe in large star-forming complexes, as discussed above for our local sample.

Very high mass ( $\sim 50 M_{\odot}$ ) stars are anticipated to be limited to massive (bright) clusters, whereas lower mass ccSNe progenitors ( $\sim 10 M_{\odot}$ ) will be found in clusters spanning a broad range of masses. The former are typically found in large (bright) star-forming complexes (e.g. Carina Nebula, 30 Doradus). Therefore, the higher frequency for H-deficient ccSNe in bright regions of their hosts with respect to H-rich ccSNe does suggest that a non-negligible fraction of Type Ib and especially Ic ccSNe originate from higher mass stars than Type II ccSNe. In reality, a mixture of close binaries and higher mass single stars is likely to be responsible for Type Ib/c ccSNe (Bissaldi et al. 2007; Smith et al. 2011).

### 5.3 Long gamma-ray bursts

From an analysis of high-redshift galaxies, Fruchter et al. (2006) revealed that long GRBs ( $\langle z \rangle = 1.25$ ) were also strongly biased towards the brightest part of their hosts, in contrast to ccSNe ( $\langle z \rangle = 0.63$ , most presumably Type II-P) which merely traced the light from their hosts.

One significant difference between the low-redshift Kelly et al. (2008) SN study and the high-redshift GRB study of Fruchter et al. (2006) is that hosts of the former are relatively high-mass, metal-rich spirals, while those of the latter are low-mass, metal-poor dwarfs. In normal star-forming galaxies the cluster mass distribution follows a power law with index  $-2$ , albeit truncated at high-mass depending upon the star formation intensity ( $\Sigma_R$ ; Gieles 2009). Consequently, similar absolute numbers of stars are formed in low-mass ( $M_{\text{cl}} \sim 10^2 M_{\odot}$ ), intermediate-mass ( $\sim 10^3 M_{\odot}$ ) and high-mass ( $\sim 10^4 M_{\odot}$ ) clusters, albeit with the former deficient in stars at the extreme upper end of the IMF.

This star cluster mass function is repeated in nearby dwarf galaxies (Cook et al. 2012), but galaxy-wide triggers may induce intense, concentrated bursts of star formation (e.g. NGC 1569; Hunter et al. 2000), leading to disproportionately numerous massive star clusters

**Table 8.** Summary of expected association between H II regions and ccSNe (+ long GRBs) in host galaxies of differing star formation intensities ( $\Sigma_R$ ), following Kennicutt et al. (1989) and Gieles (2009). Star formation intensities are obtained from  $R_{25}$  (spirals) or  $R_D$  (irregulars). A 20 Myr duty cycle is adopted for giant H II regions, versus  $\sim 4$  Myr for isolated H II regions.

Host	Star formation intensity	$\Sigma_{R_{25}}$ ( $\Sigma_{R_D}$ ) ( $M_\odot \text{ yr}^{-1} \text{ kpc}^{-2}$ )	Cluster range ( $M_\odot$ )	Characteristic H II region	SN/GRB-H II association?	Example
Sab	Low	$4 \times 10^{-5}$	$10^{2-4}$	Isolated	$m_{B_T} \mathcal{X}$ (all types)	M31
Scd	High	$2 \times 10^{-3}$	$10^{2-6}$	Giant; isolated	$\mathcal{X}(\leq 12 M_\odot)$ , ? (12–85 $M_\odot$ ), $\checkmark(\geq 85 M_\odot)$	M101
Irr	Low	( $5 \times 10^{-3}$ )	$10^{2-4}$	Isolated	$\mathcal{X}$ (all types)	SMC
Irr	High	(1.5)	$10^{2-6}$	Giant; isolated	$\mathcal{X}(\leq 12 M_\odot)$ , ? (12–85 $M_\odot$ ), $\checkmark(\geq 85 M_\odot)$	NGC 1569

Star formation intensities: M31 (Lee et al. 2009b); M101: This work; SMC: Massey et al. (2007); NGC 1569: Kennicutt et al. (2008).

(Billett, Hunter & Elmegreen 2002; Portegies Zwart, McMillan & Gieles 2010).<sup>12</sup>

We have attempted to set out the potential association between H II regions, ccSNe (and long GRBs) for star-forming spirals and irregulars in Table 8. Here, the full spectrum of galaxy types has been distilled down to two dominant types for both spirals and irregulars, depending upon the rate of star formation, or more strictly the star formation intensity. For spiral galaxies, we quote intensities with respect to  $R_{25}$ , while the  $V$ -band scalelength  $R_D$  (Hunter & Elmegreen 2004) is used for irregulars. Of course, intensities depend upon the diagnostic used to calculate SFR (Calzetti et al. 2007; Lee et al. 2009b; Botticella et al. 2012), and very different intensities would follow from the use of alternative radii (e.g. Kennicutt et al. 2005).

From Table 8, one would not expect ccSNe to usually be associated with bright regions in low-intensity environments, such as typical early-type spirals (e.g. M31) or dwarf irregulars (e.g. SMC), owing to the scarcity of giant H II regions in such hosts. Indeed, isolated H II regions in such galaxies would rarely produce high-mass stars (recall Fig. 1a). Exceptions do exist of course, including early-type spiral galaxies that possess high star formation intensities (e.g. M81), plus abnormal regions within non-starburst irregulars such as NGC 346 in the SMC.

In contrast, the high star formation intensity of late-type spirals (e.g. M101) and starburst irregulars (e.g. NGC 1569) will produce many large, star-forming complexes. Consequently, ccSNe will frequently be associated with bright star-forming regions within their host galaxies. Of the present ccSNe sample, whose hosts are typical of high-intensity late-type spirals, 18/37 ccSNe lie within  $\sim 300$  pc of a bright ( $L(\text{H}\alpha) > 10^{38} \text{ erg s}^{-1}$ ) star-forming region. Our sample includes only two irregular galaxies, so we are unable to assess the situation for starburst versus non-starburst dwarf galaxies.

Nevertheless, we can re-assess the likelihood that long GRBs arise from moderate- ( $\sim 15 M_\odot$ ) or high- ( $\sim 50 M_\odot$ ) mass stars if the local volume is fairly representative of metal-poor star formation (Lee et al. 2009a). In the former case, long GRBs would be dominated by quiescent star formation from non-starburst dwarfs, whose H II regions would be isolated (and faint) since they would lack the high-mass clusters necessary for very massive stars, and their corresponding bright H II regions. In the latter case, long GRBs would be associated with stars formed in very massive clusters, since where localized activity takes place in dwarf galaxies, it can be very intense (Billett et al. 2002).

The tight correlation between long GRBs and the brightest regions of their hosts (Fruchter et al. 2006) does not *prove* a link

between high-mass stars and long GRBs, but it is certainly highly *suggestive*. Recall the preference for broad-lined Type Ic ccSNe towards dwarf galaxies (Arcavi et al. 2010), the broad-lined Ic-GRB connection (Woosley & Bloom 2006) plus the preference of long GRBs for metal-poor hosts (Levesque et al. 2010).

Of course, the formation of dense star clusters will lead to a significant number of high-mass runaway stars, either dynamically ejected during the formation process or at later stages after receiving a kick following an SN explosion within a close binary system (e.g. Fujii & Portegies Zwart et al. 2011). Still, the majority of high-mass runaways will remain relatively close to their birth cluster in view of their short lifetimes and typical ejection velocities of  $\sim 100 \text{ km s}^{-1}$ .

For example, the progenitor of the nearby GRB 980425/SN 1998bw was located close to another bright H II region in its (late-type) host galaxy, albeit offset by 0.8 kpc from a 30 Dor-like giant H II region (Hammer et al. 2006). Either the SN/GRB progenitor was dynamically ejected from the H II region at relatively high velocities, or it was formed in situ in a more modest star-forming region, which is comparable to the Rosette Nebula (Table 1). Evans et al. (2010) have identified VFTS #016 as a high-mass runaway from R136 in the 30 Doradus, having traversed 0.12 kpc in the 1–2 Myr since the formation of the cluster.

Therefore, from environmental considerations one can understand the preference for certain flavours of ccSNe towards the brightest regions of their host galaxies. Still, there is little predictive power regarding progenitor masses, other than potentially a high likelihood for very massive stars to produce long GRBs/broad-lined Ic ccSNe.

## 6 CONCLUSIONS

We have reexamined the immediate H II environment of ccSNe from nearby ( $\leq 15$  Mpc) low-inclination ( $\leq 65^\circ$ ), host galaxies. A total of 41 ccSNe have good position accuracy, of which ground-based  $\text{H}\alpha$  imaging is available in 39 cases. Our findings can be summarized as follows.

(i) Overall, half of the ccSNe are associated with nebular emission, in close agreement with van Dyk (1992). Separating these into Type II and Type Ib/c ccSNe, 11 of the 29 hydrogen-rich ccSNe are associated with nebular emission ( $38 \pm 11$  per cent), versus 7 of the 10 hydrogen-poor ccSNe ( $70 \pm 26$  per cent), supporting previous studies of Anderson & James (2008) and Anderson et al. (2012).

(ii) Of the 18 ccSNe associated with star-forming regions, 12 are associated with giant H II regions, with the remaining six associated with low-luminosity, extended H II regions. Overall, the mean  $\text{H}\alpha$  luminosity of star-forming regions associated with ccSNe is typical of a modest giant H II region,  $3 \times 10^{38} \text{ erg s}^{-1}$ , if we were to exclude SN 1970G which lies at the periphery of the supergiant H II region NGC 5455 within M101. Both categories have multiple sites of star

<sup>12</sup> Of course, not all dwarf galaxies are starbursting. Within the local volume ( $< 11$  Mpc) only a quarter of the star formation from dwarf galaxies is formed during starbursts (Lee et al. 2009a).

formation, and so long duty cycles ( $\sim 20$  Myr), implying only weak limits upon progenitor masses ( $\geq 12 M_{\odot}$ ).

(iii) Of the 21 ccSNe not associated with star-forming regions, only one case is coincident with a bright cluster (SN 2004dj), from which a massive progenitor ( $> 20 M_{\odot}$ ) would be expected. More detailed studies of the cluster indicate a lower progenitor mass  $< 20 M_{\odot}$  (Vinkó et al. 2006, 2009) in common with most of the other ccSNe that are not associated with a star-forming region. In a few instances, nearby giant H II regions indicate the possibility that the progenitor was a (high-mass) runaway from a putative dense star cluster.

(iv) Our primary result is that the different frequency of association with H II regions for hydrogen-rich (mostly II-P) and hydrogen-poor (Ib/c) ccSNe is attributed simply to different minimum progenitor mass thresholds,  $\sim 8$  and  $\sim 12 M_{\odot}$ , respectively, since they correspond to upper age limits of  $\sim 50$  and  $\sim 20$  Myr. Among the Type Ib/c ccSNe, only two cases lacked both nebular emission and a nearby giant H II region (SN 2002ap, SN 2003jg), favouring the interacting binary channel ( $< 20 M_{\odot}$ ).

(v) For the present sample, 8 of the ccSNe originate from early-type spirals (S0/a/b), 31 from late-type spirals (Sc/d/m) and 2 from irregulars (Im), with the majority (61 per cent) arising from high-luminosity ( $M_B < -19$  mag) hosts. Giant H II regions are common in these hosts because star formation intensities are uniformly high, whereas isolated, compact H II regions would be expected to dominate in low star formation intensity hosts. ccSNe from isolated, classical H II regions would provide firm limits upon the lifetime ( $\leq 3-5$  Myr) and mass ( $\geq 50-100 M_{\odot}$ ) of the progenitor owing to the brief lifetime of such H II regions, although this would require higher spatial resolution (*HST* or ground-based Adaptive Optics). An association between a ccSN and compact H II regions has not been observed with *HST* to date (Table 7).

(vi) We have also qualitatively re-assessed the preference for Type Ib/c towards the brightest regions of their host galaxies (Kelly et al. 2008). This is suggestive that a fraction of H-poor ccSNe originate from significantly higher mass stars than Type II ccSNe, since high-mass stars are more likely to be associated with high-mass clusters within large (bright) star-forming complexes. The preference for long GRBs towards the brightest regions of their metal-poor hosts (Fruchter et al. 2006) is also suggestive of very high mass progenitors. This is because low-intensity star-forming dwarfs do not form very high mass stars, yet dominate the overall metal-poor star formation in the local volume (Lee et al. 2009a).

## ACKNOWLEDGMENTS

I wish to thank the referee for suggestions which helped to clarify some aspects of this work. In addition, I am especially grateful to John Eldridge for alerting me to this issue, and to Mark Gieles and Rob Kennicutt for useful discussions. Janice Lee and Johan Knapen kindly provided me with electronic access to archival imaging, while Maryam Modjaz kindly provided updated SN spectral types prior to publication.

This study was based in part on observations made with (a) ESO Telescopes at the La Silla Paranal Observatory under programme IDs 067.D-0006(A), 069.B-0125(A), 069.D-0453(A), 075.D-0213(A), 380.D-0282(A) and 081.B-0289(C); (b) Gemini Observatory under programme GN-2009B-Q-4, which is operated by the Association of Universities for Research in Astronomy, Inc., under a cooperative agreement with the NSF on behalf of the Gemini partnership: the National Science Foundation (United States), the Science and Technology Facilities Council (United Kingdom), the

National Research Council (Canada), CONICYT (Chile), the Australian Research Council (Australia), Ministério da Ciência, Tecnologia e Inovação (Brazil) and Ministerio de Ciencia, Tecnología e Innovación Productiva (Argentina); (c) NASA/ESA *Hubble Space Telescope*, obtained from the data archive at the Space Telescope Institute. STScI is operated by the association of Universities for Research in Astronomy, Inc. under the NASA contract NAS 5-26555. This research has also used the facilities of the CADM operated by the National Research Council of Canada with the support of the Canadian Space Agency; (d) Isaac Newton Group Archive which is maintained as part of the CASU Astronomical Data Centre at the Institute of Astronomy, Cambridge; (e) Liverpool Telescope Data Archive, provided by the Astrophysics Research Institute at Liverpool John Moores University.

This research has made extensive use of the NASA/IPAC Extragalactic Database (NED) which is operated by the Jet Propulsion Laboratory, California Institute of Technology, under contract with the National Aeronautics and Space Administration. I also acknowledge the usage of the HyperLeda data base (<http://leda.univ-lyon1.fr>).

## REFERENCES

- Aldering G., Humphreys R. M., Richmond M., 1994, *AJ*, 107, 662  
 Allen R. J., Goss W. M., Ekers R. D., de Bruyn A. G., 1976, *A&A*, 48, 253  
 Anderson J. P., James P. A., 2008, *MNRAS*, 390, 1527  
 Anderson J. P., Haberman S. M., James P. A., Hamuy M., 2012, *MNRAS*, 424, 1372  
 Arcavi I. et al., 2010, *ApJ*, 721, 777  
 Arcavi I. et al., 2012, *ApJ*, 756, L30  
 Bartunov O. S., Tsvetkov D. Y., Filiponova I. V., 1994, *PASP*, 106, 1276  
 Bastian N., Covey K. R., Meyer M. R., 2010, *ARA&A*, 48, 339  
 Bik A., Lamers H. J. G. L. M., Bastian N., Panagia N., Romaniello M., 2003, *A&A*, 397, 473  
 Billett O. H., Hunter D. A., Elmegreen B. G., 2002, *AJ*, 123, 1454  
 Bissaldi E., Calura F., Matteucci F., Longo F., Barbiellini G., 2007, *A&A*, 471, 585  
 Bothun G. D., Thompson I. B., 1988, *AJ*, 96, 877  
 Botticella M. T., Smartt, S. J., Kennicutt R. C., Cappellaro, E., Sereno, M., Lee, J. C., 2012, *A&A*, 537, A132  
 Bresolin F., Garnett D. R., Kennicutt R. C., Jr, 2004, *ApJ*, 615, 228  
 Calzetti D. et al., 2007, *ApJ*, 666, 870  
 Calzetti D., Chandar R., Lee J. C., Elmegreen B. G., Kennicutt R. C., Whitmore B., 2010, *ApJ*, 719, L158  
 Cao L., 1998, *IAU Circ.*, 6994  
 Carignan C., Puche D., 1990, *AJ*, 100, 394  
 Chugai N. N., Utrobin V. P., 2000, *A&A*, 354, 557  
 Ciardullo R., Jacoby G. H., Tonry J. L., 1993, *ApJ*, 419, 479  
 Ciardullo R., Feldmeier J. J., Jacoby G. H., Kuzio de Naray R., Laychak M. B., Durrell P. R., 2002, *ApJ*, 577, 31  
 Clark J. S., Negueruela I., Crowther P. A., Goodwin S. P., 2005, *A&A*, 434, 949  
 Conti P. S., 1976, *Proc. 20th Colloq. Int. Ap. Liege*, p. 193  
 Conti P. S., Crowther P. A., Leitherer C., 2008, *From Luminous Hot Stars to Starburst Galaxies*. Cambridge Univ. Press, Cambridge  
 Cook D. O. et al., 2012, *ApJ*, 751, 100  
 Crockett R. M., 2009, PhD thesis, Queen's University Belfast  
 Crockett R. M. et al., 2007, *MNRAS*, 381, 835  
 Crockett R. M. et al., 2008, *ApJ*, 672, L99  
 Crowther P. A., 2007, *ARA&A*, 45, 177  
 Crowther P. A., Schnurr O., Hirschi R., Yusof N., Parker R. J., Goodwin S. P., Kassim H. A., 2010, *MNRAS*, 408, 731  
 Dalcanton J. J. et al., 2009, *ApJS*, 183, 67  
 Dale J. E., Ercolano B., Bonnell I. A., 2012, *MNRAS*, 424, 377

- Danver C. G., 1942, *Ann. Obs. Lund*, 10, 1
- de Wit W. J., Testi L., Palla F., Zinnecker H., 2005, *A&A*, 437, 247
- Dessart L., Hillier D. J., Li C., Woosley S., 2012, *MNRAS*, 424, 2139
- Ekström S. et al., 2012, *A&A*, 537, A146
- Eldridge J. J., 2012, *MNRAS*, 422, 794
- Evans N. J., II, Dunham M. M., Jørgensen J. K., 2009, *ApJS*, 181, 321
- Evans C. J. et al., 2010, *ApJ*, 715, L74
- Evans C. J. et al., 2011, *A&A*, 530, A108
- Freedman W. F. et al., 2001, *ApJ*, 553, 47
- Freeman K. C., Karlsson B., Lynga G., Burrell J. F., van Woerden H., Goss, W. M., Mebold U., 1977, *A&A*, 55, 445
- Fruchter A. S. et al., 2006, *Nat*, 441, 463
- Fryer C. L. et al., 2007, *PASP*, 119, 861
- Fujii M. S., Portegies Zwart S. F., 2011, *Sci*, 334, 1380
- Georgy C. et al., 2012, *A&A*, 542, A29
- Gieles M., 2009, *MNRAS*, 394, 2113
- Gieles M., Portegies Zwart S. F., 2011, *MNRAS*, 410, L6
- Grebel E. K., Chu Y.-H., 2000, *AJ*, 119, 787
- Hadfield L. J., Crowther P. A., Schild H., Schmutz W., 2005, *A&A*, 439, 265
- Hammer F., Flores H., Schaerer D., Dessauges-Zavadsky M., Le Floch E., Poech M., 2006, *A&A*, 454, 103
- Harayama Y., Eisenhauer F., Martins F., 2008, *ApJ*, 675, 1319
- Hunter D. A., Elmegreen B. G., 2004, *AJ*, 128, 2170
- Hunter D. A., O'Connell R. W., Gallagher J. S., Smecker-Hane T. A., 2000, *AJ*, 120, 2383
- Iwamoto K., Nomoto K., Höflich P., Yamaoka H., Kumagai S., Shigeyama T., 1994, *ApJ*, 437, L115
- James P. A., Anderson J. P., 2006, *A&A*, 453, 57
- James P. A. et al., 2004, *A&A*, 414, 23
- Jha S., Challis P., Garnavich P., Kirshner R., Calkins M., Stanek K., 1999, *IAU Circ.*, 7296
- Kamphuis J., Briggs F., 1992, *A&A*, 253, 335
- Kelly P. L., Kirschner R. P., Pahre M., 2008, *ApJ*, 687, 1201
- Kennicutt R. C., 1984, *ApJ*, 287, 116
- Kennicutt R. C., 1998, *ARA&A*, 36, 189
- Kennicutt R. C., Kent S. M., 1983, *AJ*, 88, 1094
- Kennicutt R. C., Edgar B. K., Hodge P. W., 1989, *ApJ*, 337, 761
- Kennicutt R. C., Bresolin F., Bomans D. J., Bothun G. D., Thompson I. B., 1995, *AJ*, 109, 594
- Kennicutt R. C. et al., 2003, *PASP*, 115, 928
- Kennicutt R. C., Jr, Lee J. C., Funes J. G., Sakai S., Akiyama S., 2005, in de Grijs R., González Delgado R. M., eds, *Starbursts: From 30 Doradus to Lyman Break Galaxies*. Astrophysics Space Science Library, Vol. 329, Springer, Dordrecht, p. 187
- Kennicutt R. C., Lee, J. C., Funes S. J., José G., Sakai S., Akiyama S., 2008, *ApJS*, 178, 247
- Kennicutt R. C. et al., 2009, *ApJ*, 703, 1672
- Kiewe M. et al., 2012, *ApJ*, 744, 10
- Knapen J. H. et al., 2004, *A&A*, 426, 1135
- Lada C. J., Lada E. A., 2003, *ARA&A*, 41, 57
- Langer N., 2012, *ARA&A*, 50, 107
- Larsen S. S., Richtler T., 1999, *A&A*, 345, 59
- Lee J. C., Kennicutt R. C., Funes J. G., José G., Sakai S., Akiyama S., 2009a, *ApJ*, 692, 1305
- Lee J. C. et al., 2009b, *ApJ*, 706, 599
- Leonard D. C. et al., 2002, *AJ*, 124, 2490
- Levesque E. M., Kewley L. J., Berger E., Zahid H. J., 2010, *AJ*, 140, 1557
- Li W., Fan Y., Qiu Y. L., Hu J. Y., 2001, *IAU Circ.*, 7591
- Li W., van Dyk S. D., Filippenko A. V., Cuillandre J.-C., Jha S., Bloom J. S., Riess A. G., Livio M., 2006, *ApJ*, 641, 1060
- Lopez L. A., Krumholz M. R., Bolatta A. D., Prochaska J. X., Ramirez-Ruiz E., 2011, *ApJ*, 731, 91
- Macri L. M., Stanek K. Z., Bersier D., Greenhill L. J., Reid M. J., 2006, *ApJ*, 652, 1133
- Mager V. A., Madore B. F., Freedman W. L., 2008, *ApJ*, 689, 721
- Massey P., Olsen K. A. G., Hodge P. W., Jacoby G. H., McNeill R. T., Smith R. C., Strong, S. B., 2007, *AJ*, 133, 2393
- Maund J. R., Smartt S. J., Danzinger I. J., 2005, *MNRAS*, 364, L33
- Maund J. R. et al., 2011, *ApJ*, 739, L37
- Mazzali P. A. et al., 2002, *ApJ*, 572, L61
- Mazzali P. A. et al., 2007, *ApJ*, 670, 592
- McNaught R. H., Waldron D., 1986, *IAU Circ.*, 4261
- Méndez B., Davis M., Moustakas J., Newman J., Madore B. F., Freedman W. L., 2002, *AJ*, 124, 213
- Meurer G. R. et al., 2006, *ApJSS*, 165, 307
- Moustakas J., Kennicutt R. C., Jr, 2006, *ApJS*, 164, 81
- Murphy M. T., Bessell M. S., 2000, *MNRAS*, 311, 741
- Panagia N., Romaniello M., Scuderi S., Kirschner R. P., 2000, *ApJ*, 539, 197
- Pennington R. L., Talbot R. J., Jr, Dufour R. J., 1982, *AJ*, 87, 1538
- Pflamm-Altenburg J., Weidner C., Kroupa P., 2007, *ApJ*, 671, 1550
- Podsiadlowski P., 1992, *PASP*, 104, 717
- Podsiadlowski P., Joss P. C., Hsu J. J. L., 1992, *ApJ*, 391, 246
- Portegies Zwart S. F., McMillan S. L. W., Gieles M., 2010, *ARA&A*, 48, 431
- Porter A. C., 1993, *PASP*, 105, 1250
- Rumstay K. S., Kaufman M., 1983, *ApJ*, 274, 611
- Ryder S. D., Dopita M. A., 1993, *ApJS*, 88, 415
- Sakai S., Ferrarese L., Kennicutt R. C., Jr, Saha A., 2004, *ApJ*, 608, 42
- Sánchez S. F., Rosales-Ortega F. F., Kennicutt R. C., Johnson B. D., Diaz A. I., Pasquali, A., Hao, C. N., 2011, *MNRAS*, 410, 313
- Schaefer B. E., 2008, *AJ*, 135, 112
- Schlafly E. F., Finkbeiner D. P., 2011, *ApJ*, 737, 103
- Schlegel D. J., Finkbeiner D. P., Davis M., 1998, *ApJ*, 500, 525
- Schmidt B. P., Kirshner R. P., Eastman R. G., Phillips M. M., Suntzeff N. B., Hamuy M., Maza J., Aviles R., 1994, *ApJ*, 432, 42
- Schnurr O., Casoli J., Chené A.-N., Moffat A. F. J., St Louis N., 2008, *MNRAS*, 389, L38
- Smartt S. J., 2009, *ARA&A*, 47, 63
- Smartt S. J., Eldridge J. J., Crockett R. M., Maund J. R., 2009, *MNRAS*, 395, 1409
- Smith N., 2008, in Bresolin F., Crowther P. A., Puls J., eds, *Proc. IAU Symp. 250. Massive Stars as Cosmic Engines*. Astron. Soc. Pac., San Francisco, p. 193
- Smith M. C., Leiton R., Pizarro S., 2000, in Allion D., Olsen K., Galaz G., eds, *ASP Conf. Ser. Vol. 221, Stars, Gas and Dust in Galaxies: Exploring the Links*. Astron. Soc. Pac., San Francisco, p. 83
- Smith N., Li W., Filippenko A. V., Chornock R., 2011, *MNRAS*, 412, 1522
- Sramek R. A., Panagia N., Weiler K. W., 1984, *ApJ*, 285, L59
- Stockdale C. J. et al., 2002, *IAU Circ.*, 8018
- Thim F., Tammann G. A., Saha A., Dolphin A., Sandage A., Tolstoy E., Labhardt L., 2003, *ApJ*, 590, 256
- Tonry J. L., Dressler A., Blakeslee J. P., Ajhar E. A., Fletcher A. B., Luppino G. A., Metzger M. R., Moore C. B., 2001, *ApJ*, 546, 681
- Tully R. B., Rizzi L., Shaya E. J., Courtois H. M., Makarov D. I., Jacobs B. A., 2009, *AJ*, 138, 323
- Vacca W. D., Conti P. S., 1992, *ApJ*, 401, 543
- van Dyk S. D., 1992, *AJ*, 103, 1788
- van Dyk S., Hamuy M., Filippenko A. V., 1996, *AJ*, 111, 2017
- Vazquez R. A., Baume G., Feinstein A., Prado P., 1996, *A&AS*, 116, 75
- Vinkó J. et al., 2006, *MNRAS*, 369, 1780
- Vinkó J. et al., 2009, *ApJ*, 695, 619
- Walborn N. R., 2010, in Leitherer C., Bennett P. D., Morris P. W., van Loon J. Th., eds, *ASP Conf. Ser. Vol. 425, Hot and Cool: Bridging Gaps in Massive-Star Evolution*. Astron. Soc. Pac., San Francisco, p. 45
- Walborn N. R., Blades J. C., 1997, *ApJS*, 112, 457
- Wang J. et al., 2011, *ApJS*, 194, 11
- Weidner C., Kroupa P., 2006, *MNRAS*, 365, 1333
- Wilking B. A., Lada C. J., Young E. T., 1989, *ApJ*, 340, 823
- Woosley S. E., Bloom J. S., 2006, *ARA&A*, 44, 507
- Yoon S.-C., Woosley S. E., Langer N., 2010, *ApJ*, 725, 940
- Yoon S.-C., Gräfener G., Vink J. S., Kozyreva A., Izzard R. G., 2012, *A&A*, 544, L11

**APPENDIX A: DESCRIPTION OF INDIVIDUAL CCSNE ENVIRONMENTS**

A brief description of the immediate environment of each ccSNe in its host galaxy is presented, together with ground-based net H $\alpha$  and continuum images on a (projected) scale of  $1 \times 1$  kpc ( $2 \times 2$  kpc or  $4 \times 4$  kpc in some cases). An illustrative case is included below, with discussions and figures for other ccSNe presented in the online only Appendix A.

**A1 SN 1923A in M83**

SN 1923A (II-P) was discovered in 1923 May, 2.1 arcmin ( $0.33 R_{25}$ ) NE from the centre of M83 (NGC 5236; Pennington et al. 1982). The low inclination of M83 implies negligible projection effects, so this corresponds to 3.0 kpc for the adopted 4.9 Mpc distance to M83 (1 arcsec closely approximates to 25 pc). As illustrated in Fig. A1, the SN position is immediately to the south of a bright, extended, star-forming region in our VLT/FORS2 imaging from 2002 June, # 59 from the H II region catalogue of Rumstay & Kaufman (1983). A

giant H II region within the complex lies 4 arcsec (100 pc) to the N of the SN position, although extended emission extends significantly closer in our VLT/FORS2 imaging. The luminosity of the H II region is comparable to N66 (SMC), for which we measure  $1.7 \times 10^{38}$  ( $7.8 \times 10^{38}$ ) erg s $^{-1}$  using a 1 arcsec (4 arcsec) radius aperture. *HST* WFC3 imaging (GO 11360; PI R.W. O’Connell) using the F657N filter provides a higher spatial view of the region, and reveals several point sources within the error circle of the SN position, plus a faint arc coincident with the SN that extends further to the SW. A more extended star-forming region, #79 from Rumstay & Kaufman (1983), lies  $\sim 23$  arcsec (0.55 kpc) to the W, at the edge of Fig. A1.

**APPENDIX B: CORE-COLLAPSE SNe LOCATED AT DISTANCES OF 15–20 Mpc**

Basic properties of ccSNe host galaxies located at distances of 15–20 Mpc (from Tully et al. 2009). Separate tables are presented for low-inclination ( $\leq 65^\circ$ ) hosts for which accurate ccSNe positions

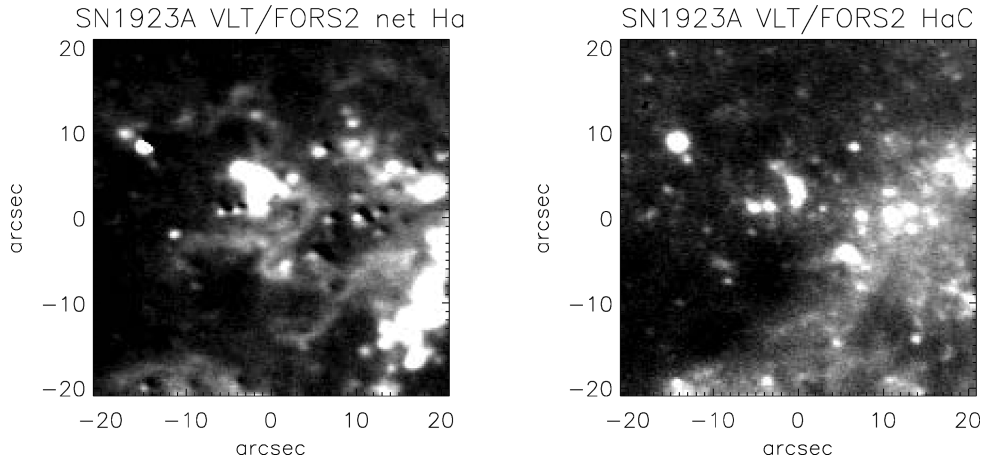


**Figure A1.** Left: VLT/FORS2 net H $\alpha$  image (from Hadfield et al. 2005) showing the nebular environment of SN 1923A (at centre of image, Class 5). The  $42 \times 42$  arcsec $^2$  field of view projects to  $1 \times 1$  kpc $^2$  at the 4.9 Mpc distance of M83; right: continuum image ( $\lambda_c = 6665$  Å). North is up and east is to the left for these and all subsequent images.

**Table B1.** Basic properties of host galaxies of ccSNe, drawn from RC3 or HyperLeda, for which EDD distances lie in the range 15–20 Mpc, restricted to low-inclination ( $\leq 65^\circ$ ) hosts for which accurate ccSNe positions are known. SN imposter hosts are also omitted (e.g. SN 2003gm in NGC 5334; Smartt et al. 2009)

PGC	M	NGC	UGC	Type	$cz$ (km s $^{-1}$ )	$i$	$d$ (Mpc)	Ref	ccSNe	
02081		157		SAB(rs)bc	1652	61.8	20.0	1	2009em	
03572		337		SB(s)d	1648	50.6	19.5	$\pm$ 1.6	1	2011dq
06826		701		SB(rs)c	1831	62.4	19.3	$\pm$ 3.8	1	2004fc
09236		918	01888	SAB(rs)c?	1507	57.6	16.1	$\pm$ 3.2	1	2009js
09846		991		SAB(rc)s	1532	28.1	17.3	$\pm$ 1.1	1	1984L
10464		1084		SA(s)c	1407	49.9	17.3	$\pm$ 1.1	1	1996an, 1998dl, 2009H
11479		1187		SB(r)c	1390	44.3	18.9	$\pm$ 2.6	1	1982R, 2007Y
13179		1365		SB(s)b	1636	62.7	18.0	$\pm$ 1.8	1	1983V, 2001du
14617		– ESO G420-G009 –		SB(s)c	1367	41.7	17.7	$\pm$ 1.2	2	2003bg
14620		1536		SB(s)c pec?	1217	44.8	18.0	$\pm$ 1.0	1	1997D
15850		1640		SB(r)b	1604	17.2	16.8	$\pm$ 3.5	1	1990aj
29469			05460	SB(rs)d	1093	39.7	20.0		1	2011ht
31650		3310	05786	SAB(r)bc pec	993	16.1	20.0		1	1991N
32529		3423	05962	SA(s)cd	1011	32.1	17.0	$\pm$ 2.5	1	2009ls
34767		3631	06360	SA(s)c	1156	34.7	18.0		1	1964A, 1965L, 1996bu
36243		3810	06644	SA(rs)c	992	48.2	16.3	$\pm$ 1.7	1	1997dq, 2000ew
37229		3938	06856	SA(s)c	809	14.1	17.1	$\pm$ 0.8	1	1961U, 1964L, 2005ay

Table B1 – continued

PGC	M	NGC	UGC	Type	$cz$ (km s <sup>-1</sup> )	$i$	$d$ (Mpc)		Ref	ccSNe
37290		3949	06869	SA(s)bc?	800	56.5	17.1	± 0.8	1	2000db
37306		3953	06870	SB(r)bc	1052	62.1	17.1	± 0.8	1	2006bp
37735			06983	SB(rs)cd	1082	37.4	17.1	± 0.8	1	1994P
37845		4030	06993	SA(s)bc	1465	47.1	19.5	± 1.5	1	2007aa
38068		4051	07030	SAB(rs)bc	700	30.2	17.1	± 0.8	1	<i>1983I, 2003ie, 2010br</i>
39578	99	4254	07345	SA(s)c	2407	20.1	1.8	± 0.8	1	<i>1967H, 1972Q, 1986I</i>
40001	61	4303	07420	SAB(rs)bc	1566	18.1	17.6	± 0.9	1	<i>1926A, 1961I, 1964F, 1999gn, 2006ov, 2008in</i>
40153	100	4321	07450	SAB(s)bc	1571	23.4	15.2	± 1.5	1	1979C
40745		4411B	07546	SAB(s)cd	1272	26.6	16.8	± 0.8	1	1992ad
41050		4451	07600	Sbc?	864	53.6	16.8	± 0.8	1	1985G
41746		4523	07713	SAB(s)m	262	25.1	16.8	± 0.8	1	1999gq
42833		4651	07901	SA(rs)c	788	49.5	16.8	± 0.8	1	1987K, 2006my
43321		4699		SAB(rs)b	1394	42.6	15.3	± 1.0	1	1983K
43972		4790		SB(rs)c?	1344	58.8	15.3	± 1.0	1	2012au
44797		4900	08116	SB(rs)c	960	19.0	15.6	± 1.0	1	1999br
45948		5033	08307	SA(s)c	875	64.6	18.5	± 1.1	1	1985L, 2001gd
52935		– Arp 261 –		IB(s)m pec	1856	58.8	20		1	1995N
58827		6207	10521	SA(s)c	852	64.7	18.1	± 2.1	1	2004A
59175		6221		SB(s)c	1499	50.9	15.6	± 1.7	1	1990W
70094		– IC 5267 –		SA0/a(s)	1712	48.4	18.7	± 1.6	1	2011hs

1: Tully et al. (2009), 2: NED (Virgo + GA + Shapley).

are known (Table B1) and high-inclination hosts and ccSNe whose coordinates are imprecisely known (Table B2, online only).

## SUPPORTING INFORMATION

Additional Supporting Information may be found in the online version of this article.

**Appendix A.** Description of individual ccSNe environments.

**Table B2.** Basic properties of host galaxies of ccSNe, drawn from RC3 or HyperLeda, for which EDD distances lie in the

range 15–20 Mpc, restricted to high inclination ( $\geq 65^\circ$ ) hosts and ccSNe whose coordinates are imprecisely known (in italics). SN imposters are omitted ([http://mnras.oxfordjournals.org/lookup/suppl/doi:10.1093/mnras/sts145/-/ DC1](http://mnras.oxfordjournals.org/lookup/suppl/doi:10.1093/mnras/sts145/-/DC1)).

Please note: Oxford University Press are not responsible for the content or functionality of any supporting materials supplied by the authors. Any queries (other than missing material) should be directed to the corresponding author for the article.

This paper has been typeset from a  $\text{\TeX}/\text{\LaTeX}$  file prepared by the author.